AIMS Materials Science, 11(2): 256–294.
DOI: 10.3934/matersci.2024015
Received: 12 August 2023
Revised: 07 January 2024
Accepted: 17 January 2024
Published: 07 March 2024

http://www.aimspress.com/journal/Materials

Research article

Performance evaluation of hybrid biodegradable oils as a lubricant during cylindrical turning of AISI 304 austenitic stainless steel

Rasaq Kazeem[1,2,*], Tien-Chien Jen[2], Godwin Akande[3], Stephen Akinlabi[4] and Esther Akinlabi[4]

[1] Department of Mechanical Engineering, University of Ibadan, Ibadan, 200005, Nigeria
[2] Department of Mechanical Engineering Science, University of Johannesburg, Auckland Park, Johannesburg, 2006, South Africa
[3] Department of Automotive Engineering, University of Ibadan, Ibadan, 200005, Nigeria
[4] Department of Mechanical and Construction Engineering, Faculty of Engineering and Environment, Northumbria University, Newcastle, NE1 8ST, United Kingdom

* **Correspondence:** Email: kazeemadebayo85@yahoo.com; Tel: +234-8033-877-073.

Abstract: In the engineering sector, machining plays a significant role. The ability of the cutting zone to dissipate heat has grown in importance for the machining industry's sustainability. Government legislation is pushing the industry to use fewer conventional lubricants as concerns about the effects on the environment and human health grow. This shifts attention to Minimum Quantity Lubrication (MQL) and biodegradable oils. The purpose of this study is to show how well two vegetable oils, in their raw forms, perform as cutting fluids during the MQL turning process of AISI 304 stainless steel. Each vegetable oil's physiochemical and lubricating qualities were examined separately. After that, the two oils that comprised the hybrid vegetable oil were blended at a ratio of 0.5:0.5. During machining with an external threading tool, the hybrid vegetable oil was compared to its equivalent mineral-based oil in terms of cutting temperature and surface roughness. The Taguchi L9 orthogonal array was used in the study. According to the data, the cutting temperature was lowest when cutting with mineral oil, and highest when cutting with a hybrid mixture. In general, the mineral oil produced a reduced surface roughness compared to the vegetable oil mixture by about 68.6%. The combo of palm kernel and yellow orleander oil marginally outperformed mineral by about 2.3% when it came to cutting temperature. The significance of this study is to develop a more sustainable and environmentally friendly lubricants for industrial applications.

Keywords: AISI 304 steel; mineral oil; palm kernel oil; vegetable oil; yellow orleander oil

1. Introduction

The interaction of tools, workpieces, and chips during the cutting process generates heat [1]. Heat, in general, has a direct impact on machining output and manufacturing costs, yet heat is an unavoidable phenomenon [2]. As a result, it is critical to investigate the characteristics and mechanisms of heat during machining processes. The tool conducts the cutting action during the machine operation by overcoming the shear strength of the workpiece [3]. This causes the workpiece to get extremely heated, which causes a highly confined thermomechanical coupled distortion in the shear region [4]. The flow of the workpiece, fracture, and the stress-strain relationship are all significantly impacted by temperature in the cutting area. In general, when the temperature rises, the workpiece ductility rises and its strength falls [5]. During the orthogonal cutting process, heat is produced in three different areas. First, plastic work at the shear plane causes heat to be produced in the primary distortion zone. Extremely high temperatures brought on by the local heating in this area weaken the material and permit further distortion [6]. Second, heat develops in the secondary deformation zone as a result of the work required to distort the chip and overcome sliding friction at the tool-chip interface area. Third, the heat released in the tertiary distortion area, at the tool-workpiece interface, is caused by the work done to overcome friction, which occurs when the tool flank face rubs against the freshly machined surface of the workpiece [7]. The primary and secondary zones' heat generation and temperatures are primarily dependent on the cutting circumstances, but the tertiary zone's heat generation is heavily impacted by tool flank wear. The heat developed cannot be eliminated, but it can be minimized by using one of two approaches: (i) accurate parameter selection for cutting i.e., spindle speed (SS), depth of cut (DC), and feed rate (FR), and (ii) accurate selection of cutting fluids.

Numerous scholars have examined the impact of cutting parameters on diverse machining characteristics, including but not limited to surface roughness (SR), cutting force (CF), cutting temperature (CT), machine sound level, and machine vibration rate. The impact of altering machining settings on the turning of SR and material removal rate (MRR) for ±30° filament-wrapped glass fiber reinforced polymer during dry cutting operations with coated tungsten carbide inserts was investigated by Kini and Chincholkar [8]. Using the empirical formulae, contour graphs of the SR and MRR under various machining circumstances were produced. An overlaying contour graph facilitates the determination of the roughness iso-value for various MRR values. Moganapriya et al. [9] investigated the effect of cutting settings on the MRR and SR of a TiAlN/WC-C, TiAlN coated tool used in computerized numerical control (CNC) turning of AISI 1015 mild steel. The coating material (TiAlN/WC-C) was shown to have a substantial influence on the output parameters. To effectively remove AISI P20, Daniyan et al. [10] devised the milling method to maximize the effects of machining parameters, including the width of the cut, cutting force, DC, and FR. Response surface methodology (RSM) and the entire Abaqus environment were used to finish the numerical design. A predictive model that links the rate of material removal as a function of the independent machining parameters was developed as a consequence of the results analysis. Okokpujie et al. [11] conducted an experimental assessment with multi-objective optimization of the machining factors on end-milling of AL8112 alloy utilizing copra oil-based multi-walled carbon nanotube nano-lubricant to resolve the machining parameters and

material adhesion. The multi-objective optimization result reveals that the optimized machining factors resulted in a minimum SR of 1.16 m, a maximum MRR of 52.1 mm^3/min, and a minimum CF of 33.75 N. Cakir [12] investigated SR, machine current, and sound level in the non-coolant turning of hardened AISI S1 steel. The method of full factorial design of experiment was used. The study used three distinct cutting speeds (175, 155, 135 m/min), FRs (0.135, 0.090, 0.045 mm/rev), and DCs (0.12, 0.08, 0.04 mm). The FR was discovered to be the most efficient cutting variable on all output variables as a result of the investigation. Tekner and Yeşlyurt [13] studied the cutting characteristics of AISI 304 austenitic stainless steel during turning to process sound. The optimal cutting speed and FR were established using flank wear, chip shape, built-up edge, machined SR, and power consumption. The cutting speed of 165 m/min and the FR of 0.25 mm/rev produced the greatest results, and process sound evaluations supported these values. Sahinoğlu and Güllü [14] looked at the connection between SR, sound intensity, vibration, and current during the milling of CuZn39Pb3 material. The investigation demonstrated that, when the FR increased, the machine's current value, vibration, sound level, and SR all increased. Fedai [15] carried out a comparative analysis of the machinability and cutting performance when turning AISI 4340 steel under dry, Minimum Quantity Lubrication (MQL), and nano-MQL conditions. In comparison to the standard settings, they saw improvements of 13% in tool wear, 7% in current, 9% in SR, and 8% in sound intensity. They concluded that the best outcomes were obtained with nano-MQL at the lowest cutting speed and FR values. Rafighi et al. [16] investigated and optimized SR, cutting force, and sound intensity in hard turning of AISI 52100 steel. It was discovered that the feed has a significant impact on SR and cutting forces, contributing 96.3% and 13.8%, respectively. DC (53.3%) and cutting speed (40%) influenced sound intensity the most. Mia et al. [17] investigated roughness, tool wear, and MRR in MQL-assisted hard turning using a coated cemented carbide tool. Design of experiment (DOE) with Taguchi orthogonal arrays and signal-to-noise ratio optimization were used. The results demonstrated that cutting speed influenced SR, DC influenced tool wear, and FR mostly affected the material removal rate.

Mineral oil is widely used in machining to reduce CT, cutting forces, and SR. However, experts are becoming more aware of the disadvantages of mineral oil. Mineral oil exposure is responsible for nearly 80% of machine tool workers' occupational medical issues, according to researchers [18]. This cutting oil is a complex petroleum-based substance that contains hazardous compounds. When used mineral oil is improperly dumped, it affects soil and water bodies. Mineral oil is frequently discouraged by scientists and tribologists in this setting. They cannot, however, be eradicated due to the need for a lubricant in machining. As a result, the idea of employing vegetable oil as a cutting fluid in machining has evolved. Many researchers have studied various engineering materials utilizing vegetable oil as a lubricant. Yin et al. [19] carried out the interfacial lubrication properties of different vegetable oils, during MQL milling of AISI 1045 based on five vegetable oils (palm, cottonseed, soybean, castor, and peanut oils). The experimental results showed that palm oil obtained the lowest friction coefficient (0.78), milling force (Fy = 156 N, Fx = 312 N), and SR values (RSM = 0.252 mm, Ra = 0.431 μm), and the smoothest surface of the workpiece. Sharma and Sidhu [20] studied the effects of dry and near-dry machining on AISI D2 steel utilizing an environmentally benign vegetable oil as a lubricant and fully eliminating mineral and petroleum-based hazardous lubricants from the turning process. In terms of SR and work-tool interface temperature, the testing results showed that near-dry machining outperforms dry machining. Kuram et al. [21] evaluated the thrust force and SR during the drilling of AISI 304 with the HSS-E tool of five cutting fluids, three vegetable oils generated from raw and modified sunflower oils, and two industrial varieties. The experiment plan made use of a Taguchi L9 orthogonal array. The

regression method and analysis of variance (ANOVA) were used to examine the results. The impact of coconut oil on tool wear and (SR) during AISI 304 carbide tool turning was investigated by Xavior and Adithan [22]. Two different cutting fluids, an emulsion and a neat cutting oil (immiscible with water), are also being used to compare the performance of coconut oil. Based on the results, it was found that coconut oil outperformed the other two cutting fluids in terms of decreasing tool wear and enhancing surface finish. In terms of milling force, SR, and surface morphology, Bai et al. [23] assessed five common vegetable oils—cottonseed, castor, palm, peanut, and soybean—as base oils for milling Grade 45 steel. The vegetable-based oils outperformed the synthetic cutting fluid in terms of milling force and surface quality. Out of all of them, palm oil had the lowest milling force (Fy = 154 N, Fx = 309 N), falling short of synthetic cutting fluids by 13.6% and 7.76%, respectively. Saleem and Mehmood [24] documented the effectiveness of castor and sunflower oils compared to the dry approach for turning Inconel 718. Response variables were tool wear, machined surface integrity, and SR. Sunflower oil with the lowest cutting speed (30 m/min) and FR (0.168 mm/rev) combination produced the least amount of tool wear. To investigate the effects of kapok vegetable oil vs other standard oils, Shankar et al. [25] applied it during milling. Using central composite design (CCD) in RSM, the SS, DC, and FR were optimized concerning flank wear and SR, respectively. By concurrently measuring the cutting force, sound pressure, and vibration, the study also kept an eye on the state of the tool. They reported that the primary cause of flank wear and SR was the FR. It was discovered that when tools wear, cutting force, sound pressure, and vibration all increase. Sen et al. [26] used the MQL approach to test six different castor-palm oil combinations (ranging from 1:0.5 to 1:3) to enhance the lubricating behavior of vegetable oil. According to their comparison study, the optimal palm-castor volume fraction reduced SR by 8.262% and 16.146%, tool wear by 2.445% and 3.155%, and specific cutting energy by 5.459% and 7.971% when compared to the castor and palm oil mediums, respectively.

Based on the literature assessment, it appears that no researcher has employed a blend of two or more vegetable oils as a cutting lubricant during the machining process. Therefore, the purpose of this study is to investigate how the combination of palm kernel oil and yellow orleander oil affects the turning performance of AISI 304 stainless steel with an external threading tool under minimum quantity lubrication conditions. The physiochemical and lubricating characteristics of vegetable oil are enumerated. Afterward, workpiece characterization will be assessed. Next, the impact of machining parameters (SS, FR, and DC) on response variables, such as SR and CT, will be studied by employing contour and surface plots. Lastly, a summary of the experimental findings will be provided.

2. Materials and methods

2.1. Seed procurement, extraction, and characterization

In this study, two different vegetable seeds were procured from the local market in Ibadan, Nigeria for the experiment. The selected seeds considered are palm kernel seeds and yellow orleander seeds. Over 25 kg of each seed were collected dried and unshelled from the market. The seeds were further dried for three days before the milling took place. The extraction of palm kernel and yellow orleander were carried out separately at the laboratory. A cold extraction process was adopted in this study. This extracted oil through the cold press extraction method is referred to as crude vegetable oil. The extraction process was stopped when 6 L of oil was obtained from the two seeds. The pictorial views of extracted palm kernel and yellow orleander oils are shown in Figure 1a,b, respectively. Extracted

crude oils were characterized for their physiochemical and lubricity properties based on ASTM standards [27]. The physiochemical and lubrication characteristics of a substance can be utilized to detect physical risks as well as to understand or forecast its environmental fate and effects on humans [28]. In the machining experiment, six litres of palm kernel oil were blended with six liters of yellow orleander oil (i.e., 50% palm kernel oil and +50% yellow orleander oil), which makes up the hybrid vegetable oil used in this research. The mineral oil employed was SAE-40, a common petroleum-based oil used in the automobile industry.

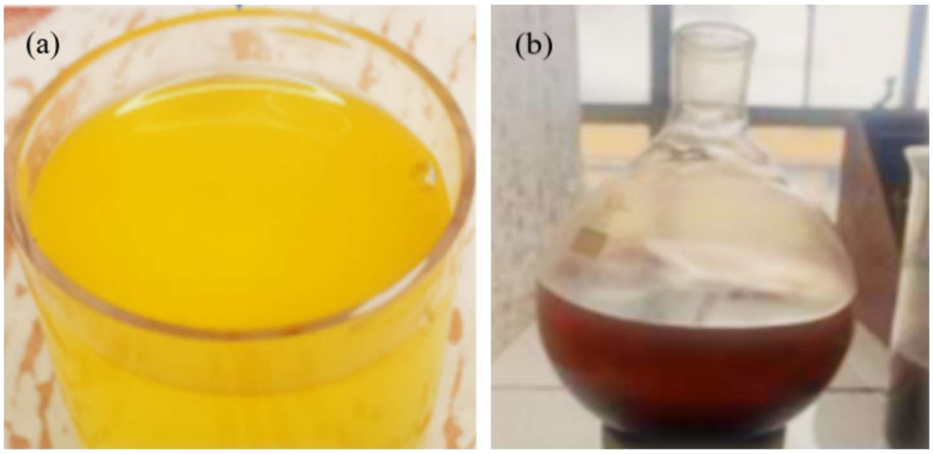

Figure 1. View of oils used in the experiments: (a) extracted palm kernel oil and (b) extracted yellow orleander oil.

2.2. Details of the workpiece

The test workpiece was taken as AISI 304 steel having a cylindrical diameter of 80 mm, while the length was 160 mm. The chemical composition and mechanical properties of the test workpiece were determined, and the results are shown in Tables 1 and 2. The relationship between the CT and SR and the cutting parameters (DC, FR, and SS) was evaluated. This study took advantage of the Taguchi design of the experiment. Using the Taguchi design approach, an $L_9(3)^3$ orthogonal array was selected, leading to a total of nine tests for each lubricating condition. The orthogonal experiment's factors and levels are shown in Table 3.

To conduct the series of experiments for this study, a three-chuck conventional lathe machine with a geared head (GH-1640ZX) was used (see Figure 2). The main technical parameters are the maximum SS of 1800 rpm, a rated power of 7.5 hp, and a voltage of 440 V. Based on their extended lifespan and the workpiece makers' comments, the external threading tools with the code DIN282 and dimensions of 20 × 20 mm were the cutting tools used for turning, as seen in Figure 3. The cutting tool has a nose radius of 0.05 mm. The MQL system consists of an oil tank, an oil-gas mixing tube, a filter, a lubricating gun, and a single-stage air compressor pressure machine. A specific amount of cutting oil is combined with compressed air at a pressure of 5 bars, and the mixture is then pumped into the cutting area. The cutting oil flow rate was estimated to be 2.4 mL/h [29].

Table 1. AISI 304 stainless steel chemical composition.

Element	Contents (%)
Sn	0.009
Al	0.0106
B	<0.0000
N	0.0083
Nb	<0.0004
V	0.004
Cu	0.100
Ni	0.0083
Mo	0.018
Cr	0.304
S	0.041
P	0.034
Mn	0.389
Si	0.172
C	0.195

Table 2. AISI 304 stainless steel mechanical properties.

Property	Value
Modulus of elasticity	196 GPa
Hardness	223 HRC
Tensile strength	512 MPa
Yield strength	207 MPa

Table 3. Factors and levels of the L_9 orthogonal experiment.

Factor	Level		
	Level 1	Level 2	Level 3
DC (mm)	0.75	1.00	1.25
FR (mm/rev)	0.10	0.20	0.25
SS (rev/min)	415	660	870

Figure 2. Pictorial view of GH-1640ZX model Lathe machine used for machining.

Figure 3. External threading tool employed for the experiment.

2.3. Measuring Equipment

2.3.1. Details of SR measurement

The average SR of the workpiece was obtained by an SR tester SRT–6100 shown in Figure 4a. In the experiment, the mean of three randomly selected values was employed along the workpiece sample's machined surface.

Figure 4. Measurement devices used in the experiment: (a) roughness test of the workpiece during turning operation, (b) photographic view of infrared thermometer.

2.3.2. Details of CT measurement

Figure 4b shows the infrared thermometer that was used to measure the CT. In an infrared thermometer, radiation is focused onto an infrared detector by a lens mechanism, which converts the energy it absorbs into an electrical signal. When modifying the temperature determined from the electrical impulse, the emissivity of the source is considered. The thermometer was carefully positioned at a distance of roughly 5 cm from the tool-workpiece contact. To get the mean result, each sample had measurements taken at three distinct points [30].

2.4. Assessment of surface and contour plots

Plots, whether surface or contour, facilitate understanding of the relationships that exist between the inputs under investigation and the outcomes. However, response surface methods and contour plots were used to study and evaluate the relationship between the cutting variables and the two responses, SR and CT. MATLAB software is used to plot the 2D contour and 3D surface plots in this investigation. Before charting on MATLAB, a software was set up for both the surface and contour plots [31].

3. Results and discussion

3.1. Evaluation of oil properties

The lubricity and physiochemical properties were carried out for each oil separately, and the results are listed in Table 4. The measured parameters have close values to those recorded in the literature. Abegunde et al. [32] obtained 925.5 and 844.2 kg/m^3 as the relative density for palm kernel oil and mineral oil, respectively. The relative density in the current study is within that of the two aforementioned values. Abegunde et al. [32] also reported 22.23 and 19.88 ℃, 24.0 and 17.67 ℃, and 232 and 195.23 ℃ as the cloud point, pour point, and fire point for palm kernel oil and mineral oil, respectively. Palm kernel oil and yellow orleander oil gave satisfactory results of parameters to a

great extent when compared with the mineral oil which serves as the control cutting fluid. There was a difference of 3%–10% between the two vegetable oils and the mineral oil used in this study. Their performances should meet up completely with mineral oil if proper lubricity additives are added. A pH value ranging between 6.4 and 6.8 for each oil denotes it is slightly acidic. This is likely to corrode the workpiece during metal cutting, though the effect might be mild because of the slight acidity. The pH is similar to what was reported by Alaba et al. [29] during an MQL turning operation of AISI 1039 steel. The two vegetable oils exist as liquids at room temperature, except that yellow orleander oil begins to solidify at temperatures slightly less than room temperature but will liquefy when exposed to sunlight or subjected to heat. The congealing of yellow orleander oil is a drawback to its lubrication tendencies. Yellow orleander cannot be used alone as a cutting fluid due to some of its properties. It would perform well in a mixture with another oil with suitable properties. This is a major reason why this study considered the mixture of palm kernel oil and yellow orleander oil as a cutting lubricant.

Table 4. Experimental results of oil characterization.

Parameter	Yellow orleander	Palm kernel oil
Color	Dark brown	Brownish-yellow
Specific gravity (kgm^{-3})	920.4	894.0
Viscosity at 100 rpm (cP)	40.8	117.6
pH	6.4	6.8
Cloud point (°C)	22.2	22.3
Pour point (°C)	20.56	21.0
Flash point (°C)	17.0	22.7
Fire point (°C)	21.0	231.0

3.2. Evaluation of machining experiments

The performances of palm kernel oil/yellow oleander oil and mineral oil when examined for possible application as cutting fluid are indicated in Table 5. The influence of the lubricating conditions on the CT and SR were further represented in Figures 5 and 6, respectively. At the spindle speed, feed rate, and DC of 870 rev/min, 0.10 mm/rev, and 1.25 mm, respectively, the palm kernel oil/yellow oleander oil and mineral oil application respectively resulted in the utmost CTs of 74.5 and 67.333 ºC. This indicated that, at these combined machining parameters, higher heat energy was absorbed by the cutting fluid during the machining process [33,34]. The high CT could be detrimental to the wear rate of the cutting tool and also affect the geometry of the chip formation and chip morphology [35–37]. Rajaguru and Arunachalam [38] and Yasir et al. [39] reported that high machining temperatures shortened the life span of the cutting tool and workpiece due to the initiation of stress corrosion cracking on the cutting tool and workpiece. However, at the spindle speed, FR and DC of 415 rev/min, 0.10 mm/rev, and 1.00 mm, respectively, the lowest CT of 38.067 °C was observed on the application of palm kernel oil/yellow oleander oil, while the lowest CT of 37.533 °C was observed at the spindle speed, FR and DC of 415 rev/min, 0.25 mm/rev, and 0.75 mm, respectively, on the application of mineral oil. The low CT at these machining parameters showed that less heat is dissipated on the cutting fluid from the abrasive effect that exists between the cutting tool and the workpiece [40,41]. At the aforementioned

machining parameters, there is a possibility of reduced friction, thus, minimizing the wear rate of the cutting tool and consequently enhancing the service life of the cutting tool [42,43].

Generally, the comparison of the CTs revealed that the application of palm kernel oil/yellow oleander oil marginally resulted in lower CTs compared to the application of mineral oil as indicated in Figure 5. For instance, the CT is lower on the application of the palm kernel oil/yellow oleander oil for experiments 1, 4, 6, 8, and 9, while the CT is marginally lower on the application of the mineral oil for experiments 2, 3, 5 and 7. This showed that the palm kernel oil/yellow oleander oil could be a superior choice of lubricant or cutting fluid for advanced machining processes, due to the possible better cooling effect the oil might offer the cutting tool and the workpiece. However, Figure 6 indicated that the application of the mineral oil as cutting fluid resulted in a reduced surface of the workpiece. All experiments 1 to 9 showed that the application of mineral oil significantly exhibited superior performance relative to the palm kernel oil/yellow oleander oil application in terms of SR. This could be attributed to the slight congealing nature of the yellow oleander oil [44]. However, the addition of some additives and oil treatments could enhance the performance of the palm kernel oil/yellow oleander oil, thus, eliminating the coagulating nature of the yellow oleander oil. As indicated in Table 4, the optimal SR (2.020 μm) was achieved at the spindle speed, feed rate, and DC of 870 rev/min, 0.25 mm/rev, and 1.00 mm, respectively. It was reported that SR in turning depends on cutting speed as an effect of built-up phenomena. With an increase in cutting speed value, SR decreases. Also, an increase in FR increases the SR due to the kinematic effect of nose radius [19, 45–48]. In the case of the mineral oil, the optimal SR of 0.838 μm was observed at the spindle speed, feed rate, and DC of 870 rev/min, 0.20 mm/rev, and 0.75 mm, respectively. The 0.838 μm was the least SR in the entire experiment. The comparable SR (0.883 μm) was observed at the spindle speed, feed rate, and DC of 415 rev/min, 0.25 mm/rev, and 1.25 mm, respectively for the mineral oil application as well. For the palm kernel oil/yellow oleander oil application, the least SR of 2.020 μm was observed at the spindle speed, FR, and DC of 870 rev/min, 0.25 mm/rev, and 1.00 mm, respectively, which is slightly less rough relative to the utmost SR of 2.050 μm observed at the spindle speed, FR, and DC of 870 rev/min, 0.20 mm/rev and 1.25 mm, respectively, with the application of palm kernel oil/yellow oleander oil. It is also worth noting that the highest SR of 6.591 μm was observed on the application of palm kernel oil/yellow oleander oil at the spindle speed, feed rate, and DC of 415 rev/min, 0.25 mm/rev and 0.75 mm, respectively. This high SR could be detrimental to the surface integrity of the workpiece and could also act as crevices for the initiation of pitting and crevice corrosion, especially in highly eco-friendly atmospheres, and chemical, petrochemical, and automobile production environments [49,50]. From the general point of view, the SR of mineral oil transcends the vegetable oil mixture by approximately 68.6%. In terms of CT, the palm kernel/yellow orleander oil mixture slightly exceeded that of mineral by roughly 2.3%.

Table 5. Experimental results of vegetable and mineral oils.

No.	SS (rev/min)	DC (mm)	FR (mm/rev)	Palm kernel/yellow orleander oil		Mineral oil	
				SR (μm)	CT (°C)	SR (μm)	CT (°C)
1	415	1.00	0.10	3.816	38.067	1.114	40.233
2	415	1.25	0.20	5.417	44.133	1.906	42.633
3	415	0.75	0.25	6.591	38.367	0.883	37.533
4	660	0.75	0.10	4.908	40.733	1.072	45.300
5	660	1.00	0.20	4.046	40.567	1.174	39.200
6	660	1.25	0.25	4.584	45.267	1.232	51.400
7	870	1.25	0.10	2.508	74.500	2.050	67.333
8	870	0.75	0.20	2.378	41.600	0.838	44.700
9	870	1.00	0.25	2.020	60.467	1.119	65.367

3.3. Effect of cutting parameters on SR and CT

The effects of cutting parameters (SS, FR, and DC) on SR and CT are displayed in Figures 7–12. The variation between FR and CT is shown in Figure 7. It was observed that the lowest CT was obtained between 0.15 and 0.20 mm/rev for mineral oil. At this point, the average temperature was approximately 41 °C. The highest CT was obtained by the mineral oil at high FR. It was noted that the CT increases as the FR increases from 0.2 mm/rev to the high FR for the two lubricating conditions that were considered. Figure 8 shows the variation between SS and CT under mineral oil and the palm kernel yellow orleander blend. SS in revolutions per minute is the number of revolutions the spindle makes in unit time. It was also noted that the CT increases as the SS increases from 415 to 660 rev/min for all the lubricants. Also, from 660 to the high SS of 870 rev/min, the CT of the lubricating oils sharply increases during the MQL machining of the AISI 304 steel. It is worth noting that increasing the SS will reduce cutting force. However, high SS will lead to high friction, thereby increasing the temperature of the cutting tool. This will lead to an increase in tool wear that will affect surface integrity. A similar trend was reported by Su et al. and Zhang et al. [51,52]. In Figure 9, the performance of the palm kernel/yellow orleander oil was far different from the mineral oil. In the vegetable oil mixed oil, the higher the SS, the lower the SR. This implies that, as the rotation of the spindle or chuck increases, the more a good surface finish will be achieved during the cutting of austenitic stainless steel with a tungsten carbide tool with palm kernel oil/yellow orleander oil mixtures [53–55]. The effectiveness of mineral oil in reducing SR was examined. At low machining SS (415 rev/min), mineral oil outperformed palm kernel/yellow orleander oil by approximately 76.2%. At 660 and 880 rev/min, mineral oil exceeded the vegetable oil blend by 74.4% and 43.5%, respectively.

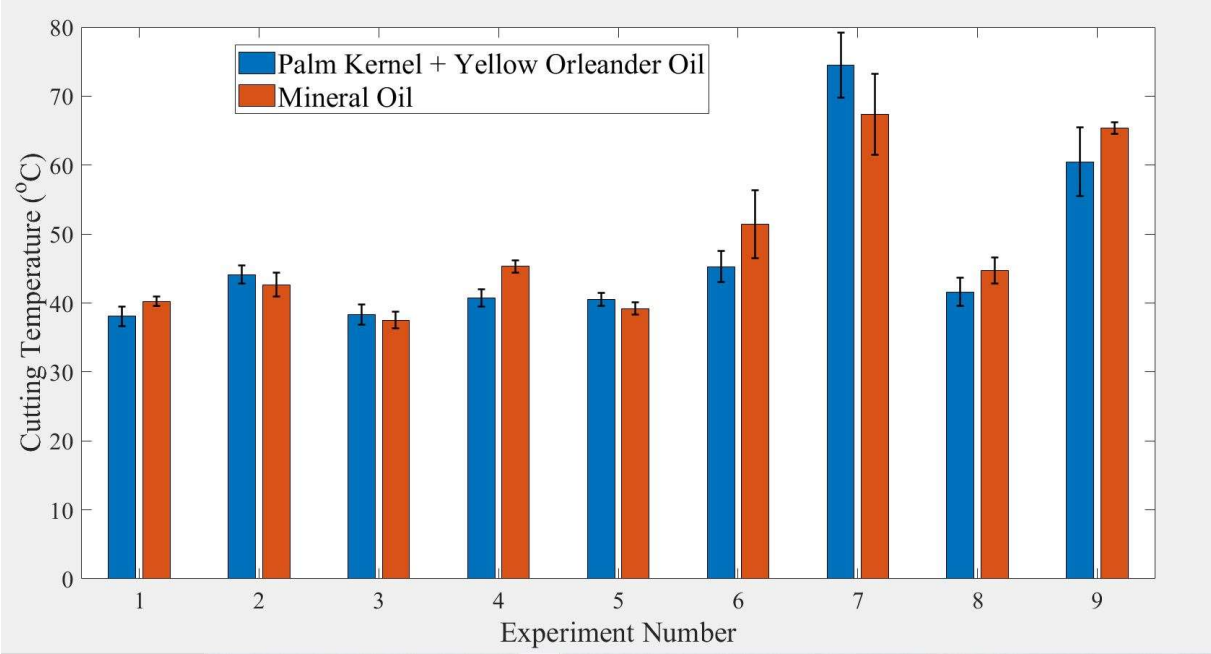

Figure 5. Effect of lubricating conditions on CT.

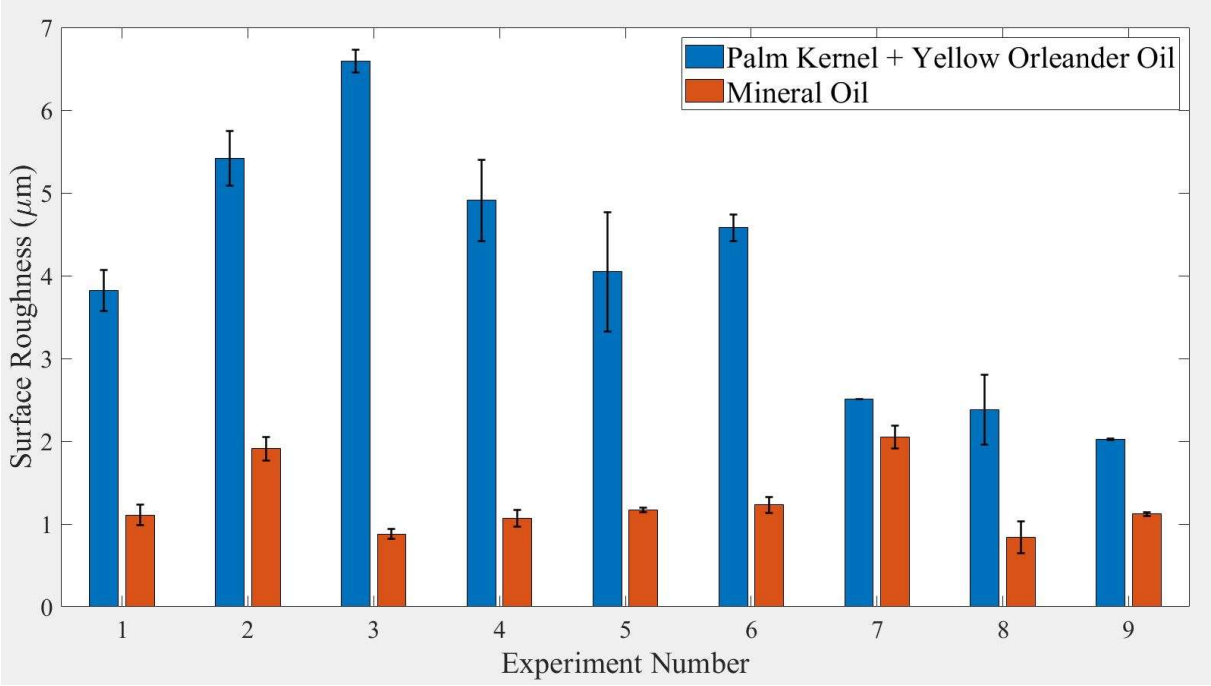

Figure 6. Effect of lubricating conditions on SR.

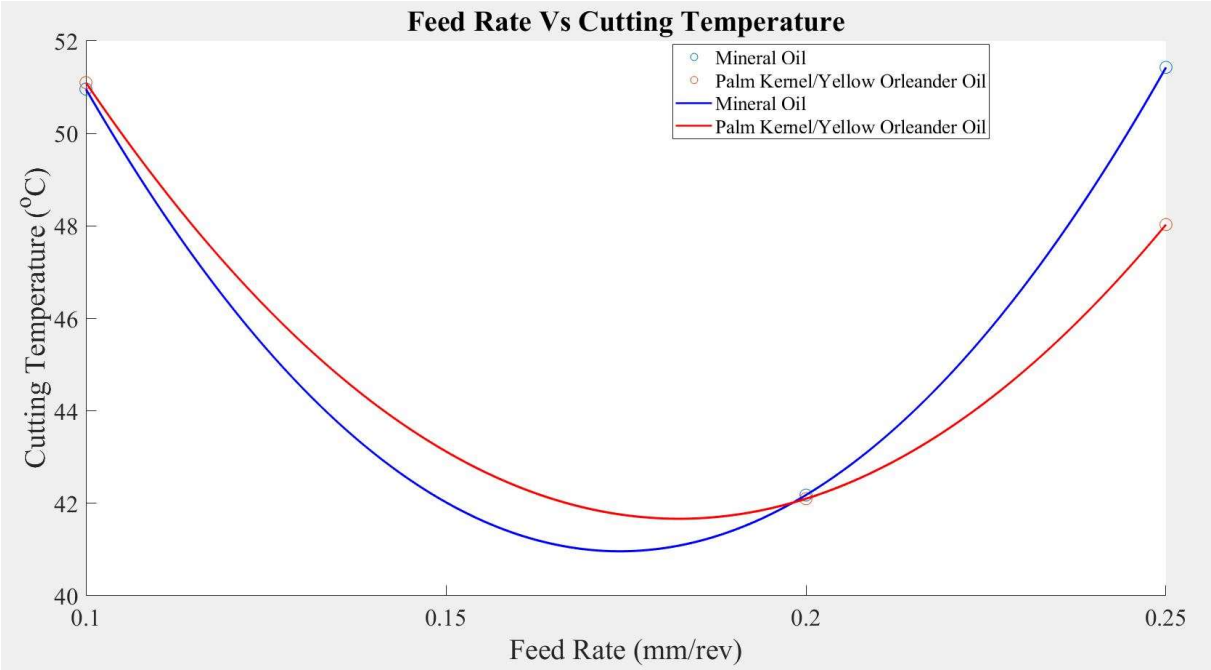

Figure 7. Effect of variation of FR on CT.

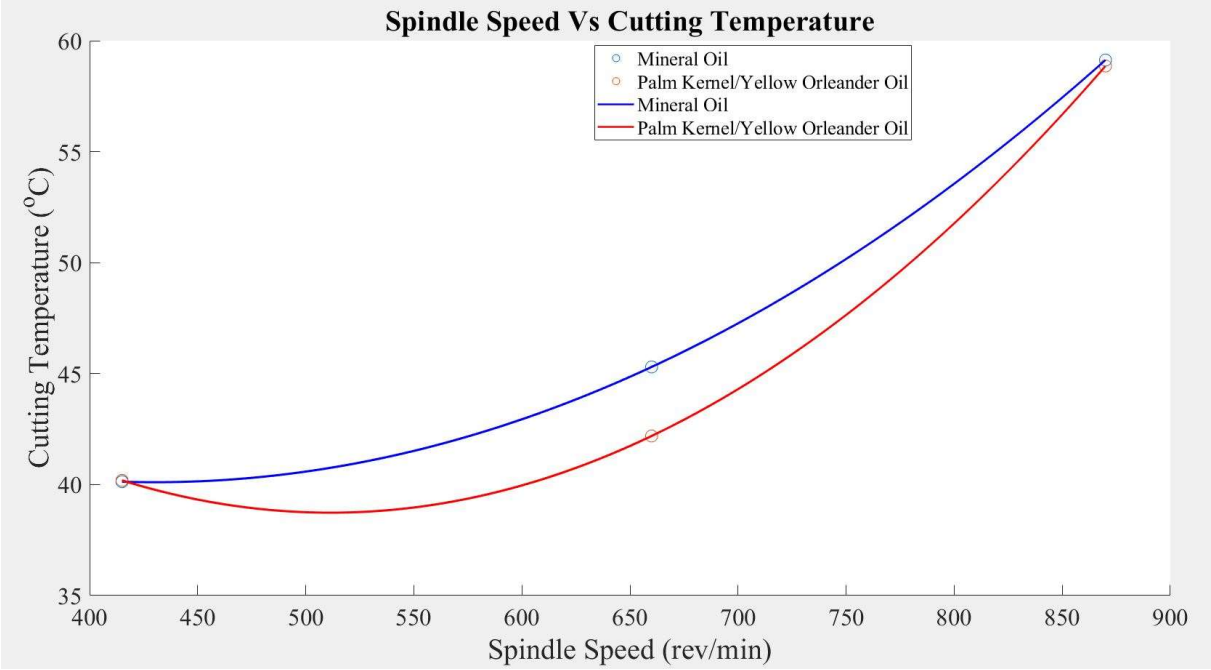

Figure 8. Effect of variation of SS on CT.

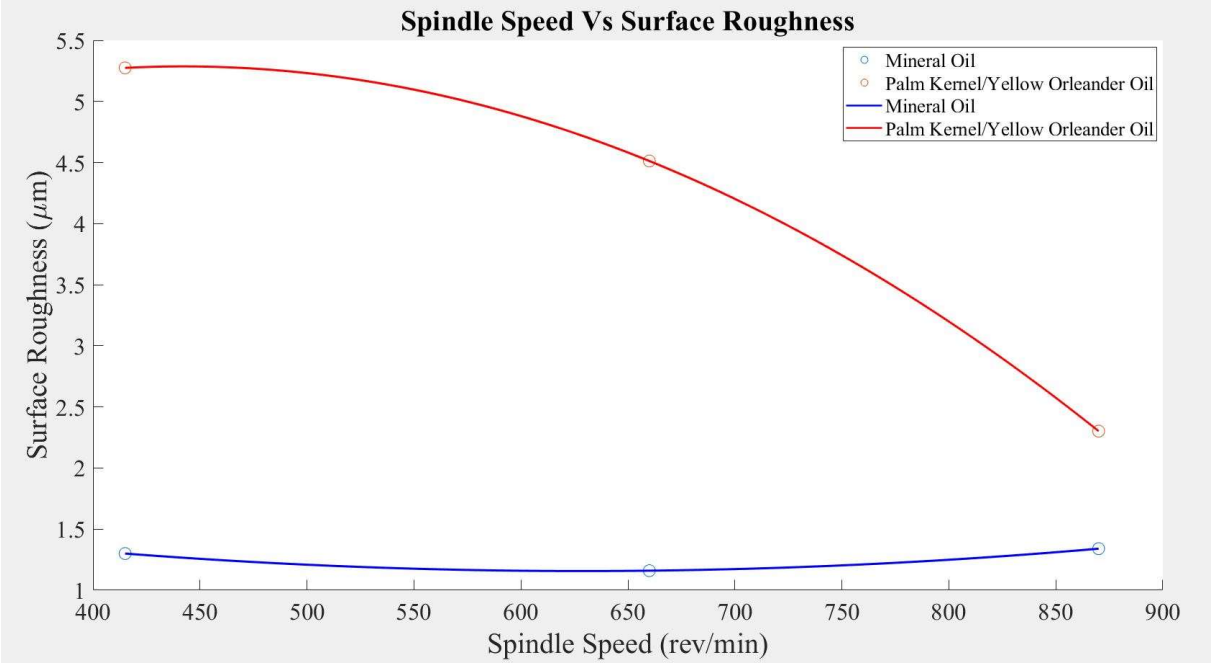

Figure 9. Effect of variation of SS on SR.

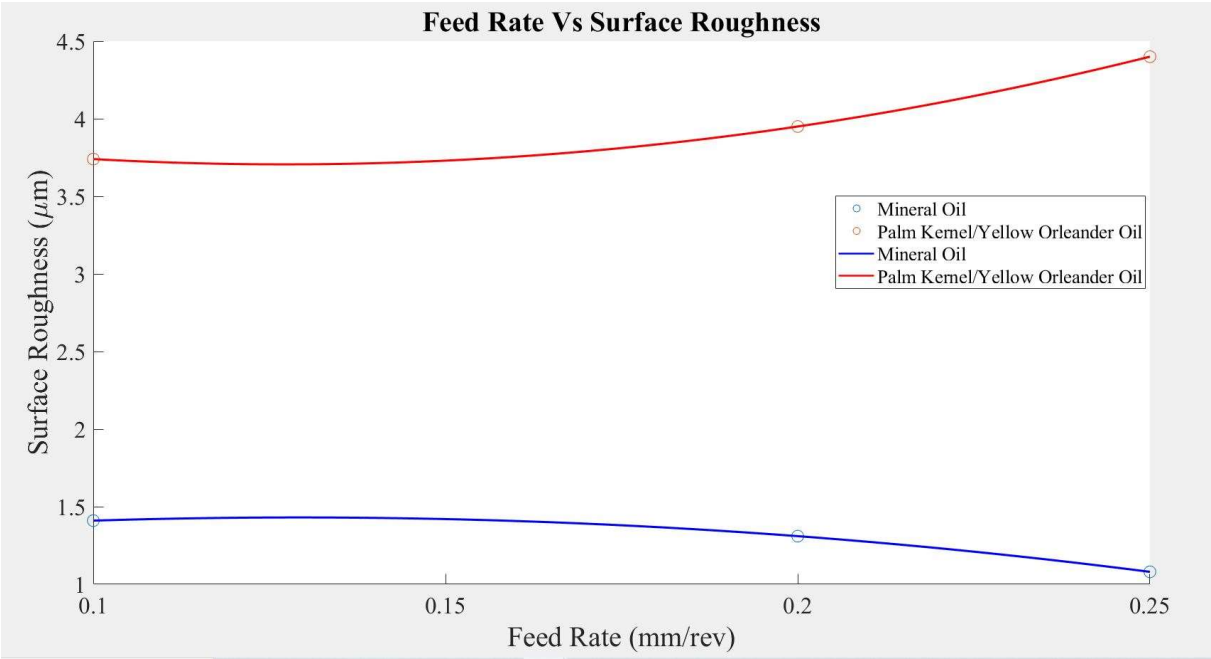

Figure 10. Effect of variation of FR on SR.

Figure 10 shows the effect of various levels of FR on the machined surface of AISI 304 steel. The pattern displayed by each of the lubricating oils was dissimilar through the levels of the FR. The palm kernel/yellow orleander oil blend exhibited an increment from low FRs of 0.10 to 0.25 mm/rev. The vegetable oil blend increased in SR from 3.75 to 4.4 µm. The mineral oil decreased in SR from 1.4 to 1.1 µm between 0.1 and 0.25 mm/rev. This showed that mineral oil reduced the SR of AISI 304 steel much better than the vegetable oil blend. A comparable scenario was reported by Majak et al. and

Xavior and Adithan [56,57]. Also, noteworthy is that mineral oil outperforms vegetable oil blends with 62.7%, 67.7%, and 75% at 0.10, 0.20, and 0.25 mm/rev FR, respectively. Figure 11 displayed the effect of various depths of cut on the machined surface for each of the two lubrication environments considered in the experiment. The SR of mineral oil increased slightly from 0.9 to 1.7 µm between DC 0.75–1.25 mm. The least SR was obtained at 0.75 mm with the conventional oil. At 0.75 mm DC, a good surface finish that would not degrade quality is significantly achieved. The highest SR was produced at 0.75 mm DC by the palm kernel-yellow orleander oil mixture. The surface quality of the machined part at 0.75 mm DC will be sacrificed. The vegetable oil blend produced a significant decrease in SR from 4.6 to about 3.35 µm, between cut depths of 0.75 and 1.0 mm. It is seen from Figure 12 that at 1.0 mm DC, more productive machining will be achieved for the vegetable oil blend. Based on Figure 5, it can be seen that there is a specific relation and pattern between CT and DC. The higher the DC, the higher the machining temperature for both mineral oil and the vegetable oil mixture. Increasing temperature patterns were observed throughout the varying DC for each lubricating oil which could lead to high wear [58]. The vegetable oil mixture increased rapidly from DC 0.75 through to 1.25 mm with its minimum and maximum temperatures measured to be 40.1 and 53 ℃, respectively. As said earlier, mineral oil moved in a similar pattern but a had very close DC at the maximum. The vegetable oil mixture surpassed the mineral oil by approximately 5% and 4% at 0.75 and 1.0 mm DC.

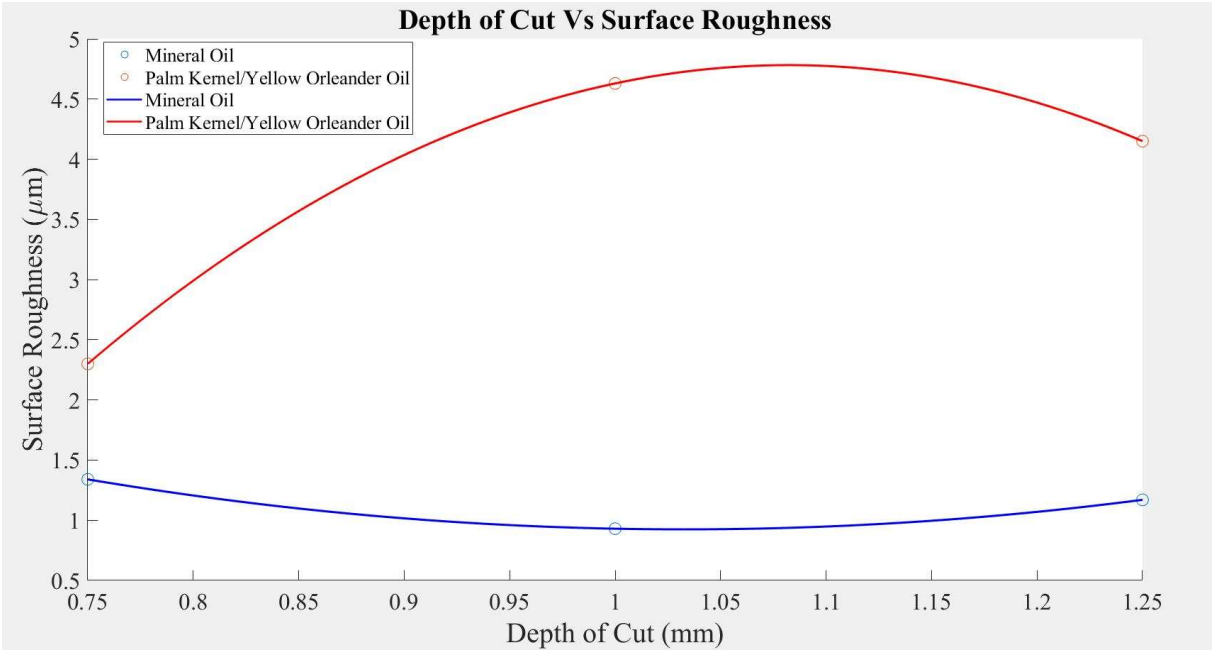

Figure 11. Effect of variation of DC on SR.

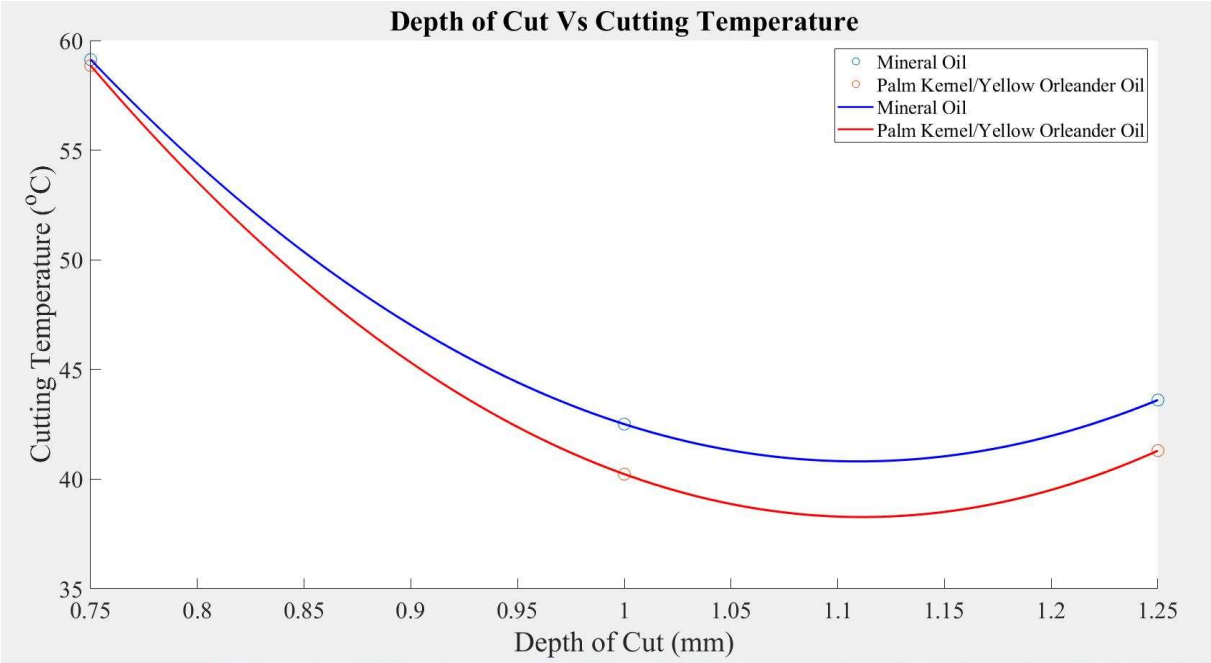

Figure 12. Effect of variation of DC on CT.

3.4. Analysis of contour and surface plots

Figure 13 illustrates a comprehensive analysis of the relationship between the independent variables, SS and DC, and their influence on the response variable, CT. Within the plot, a distinct valley can be observed, indicating the combined effect of SS ranging from 500–700 rev/min, and DC varying from 0.9–1.1 mm. Notably, the highest levels of CT are associated with SS ranging from 800–850 rev/min, paired with DC values between 1.0 and 1.25 mm. The contour lines exhibited in this plot demonstrate a non-linear trend at the valley. This suggests that the interaction between SS and DC plays a significant role in influencing the CT, surpassing the impact of either factor acting in isolation. The surface plot depicted in Figure 14 displays an irregular shape, indicating a diminishing returns relationship between the SS, DC, and CT. This irregularity suggests a non-linear correlation among these variables [59,60]. The desired optimal minimum value for the CT is approximately 38 °C, achieved when the SS is set at 600 rev/min and the SS is set at 1.0 mm. Notably, the plot demonstrates asymmetry, suggesting that CT is not equally responsive to changes in the SS and DC, regardless of the direction of adjustment. This asymmetry implies that adjustments in either parameter will not have a comparable impact on CT.

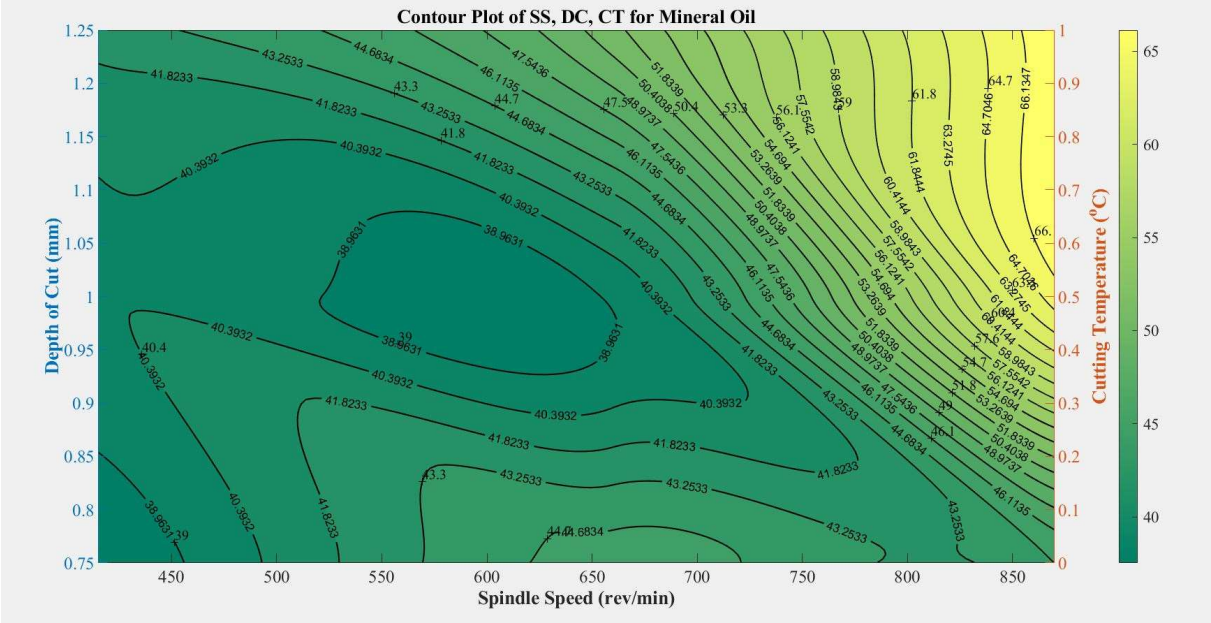

Figure 13. Contour plot of SS, DC, and CT for mineral oil.

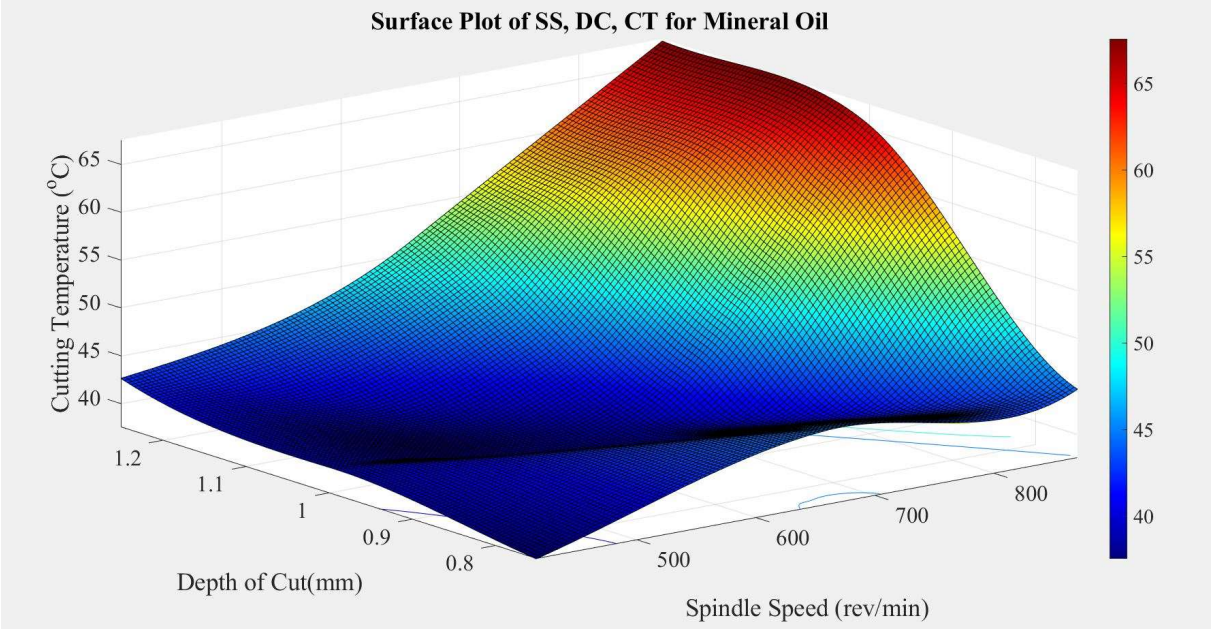

Figure 14. Surface plot of SS, DC, and CT for mineral oil.

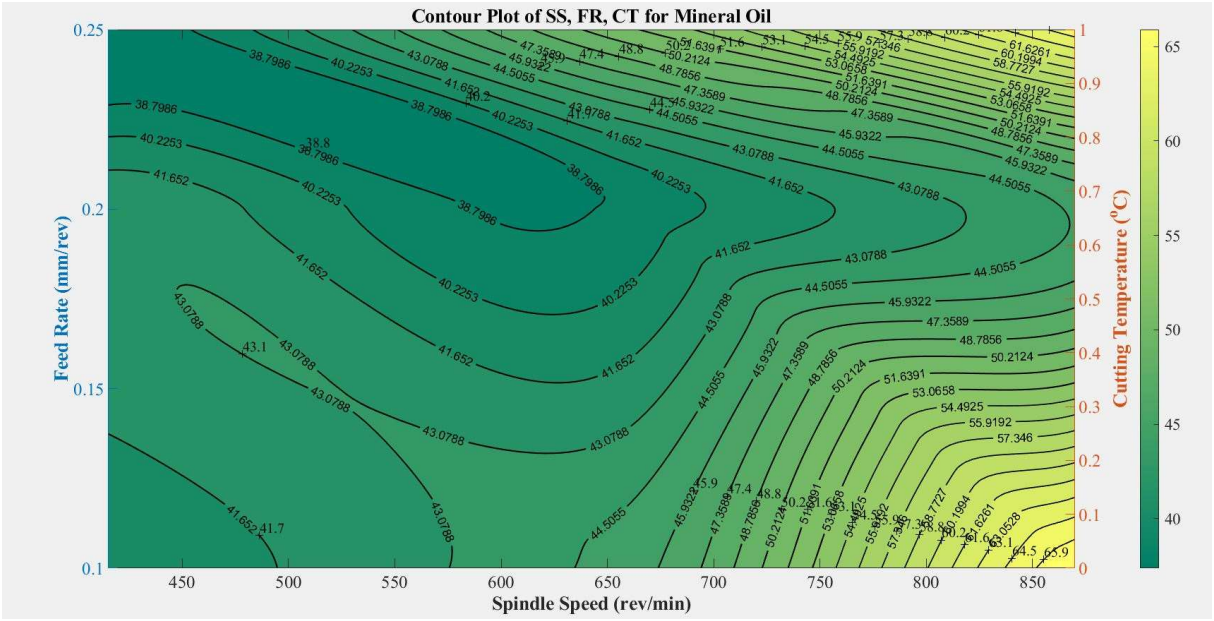

Figure 15. Contour plot of SS, FR, and CT for mineral oil.

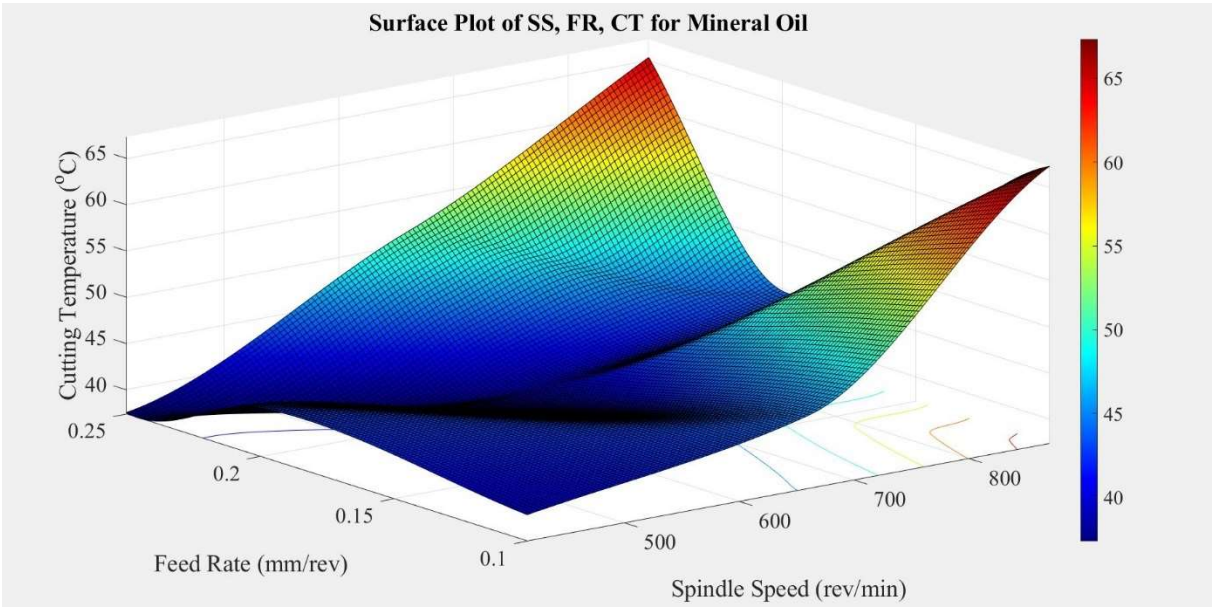

Figure 16. Surface plot of SS, FR, and CT for mineral oil.

Figure 15 illustrates the relationship between the independent variables, SS and FR, and their impact on the response variable, CT. The plot highlights that the lowest CT, less than 39 °C, is achieved when SS ranges from 450 to 650 rev/min, and FR varies between 0.2 and 0.25 mm/rev. This combination represents the valley of the plot, indicating the lowest CT values. Notably, the highest levels of CT are associated with SS ranging from 800–850 rev/min, paired with FR values between 0.1 and 0.125 mm. Additionally, CT reaches peak values with alternative SS and FR combinations of 800–850 rev/min and 0.225–0.25 mm/rev, respectively. The contour lines exhibited in this plot demonstrate a non-linear trend, indicating that changes in the SS and FR occur at varying rates within these regions. This suggests

that the interaction between SS and FR plays a significant role in influencing the CT, surpassing the impact of either factor acting in isolation [61,62]. The surface plot depicted in (Figure 16) displays an irregular shape, indicating a diminishing returns relationship between the SS, FR, and CT. This irregularity suggests a non-linear correlation among these variables. The desired optimal minimum value for the CT is approximately 38 °C, achieved when the SS is set at 550 rev/min and the FR is set at 0.225 mm/rev. Notably, the plot exhibits symmetry on the FR axis, indicating that the CT is equally sensitive to changes in the FR, regardless of the direction of adjustment. Figure 17 showcases the relationship between the independent variables, SS and DC, and their impact on the response variable, SR. Notably, the plot reveals a distinct valley representing low SR and two peaks representing high SR. The valley, characterized by an SR of approximately 1.1 μm, is achieved when the SS ranges from 800 to 850 rev/min, and the DC varies from 0.95 to 1.05 mm. Conversely, SR reaches a peak at an SS range of 400 to 500 rev/min, and a DC ranging from 1.15 to 1.25 mm. Additionally, SR reaches peak values with alternative SS and DC combinations of 800–850 rev/min and 1.15–1.25 mm, respectively. Examining the contour lines within the plot, they display curved shapes and are more concentrically spaced rather than parallel. This suggests that the interaction between SS and DC has a significant influence on altering the SR, surpassing the individual effects of each factor as also affirmed by Yeganefar et al. and Praveen et al. [63,64]. The non-linear and concentric nature of the contour lines highlights the importance of considering the combined impact of both variables when optimizing SR. Figure 18 showcases a surface plot with an irregular shape, representing the relationship between the SS, DC, and SR. This shape indicates a non-linear association among these variables. The sought-after optimal minimum value for SR, approximately 1.1 μm, is achieved by configuring the SS to 825 rev/min and the DC to 1.00 mm. It is important to note that the plot reveals asymmetry, indicating that SR does not respond equally to changes in the SS and DC, irrespective of the direction of adjustment. This asymmetry suggests that modifications in either parameter will not exert a comparable influence on CT. In Figure 19, the response variable is SR, while the independent variables are SS and FR. Two distinct peaks can be observed, representing the combinations of SS and FR that yield the highest SR. The first peak, with an SR of approximately 1.85 μm, occurs when the SS ranges from 400 to 500 rev/min and the FR ranges from 0.175 to 0.225 mm/rev. The second peak, with an SR of about 1.9 μm, is achieved with an SS ranging from 800 to 850 rev/min and an FR ranging from 0.1 to 0.125 mm/rev. Two valleys can also be observed, representing the combinations of SS and FR that yield the lowest SR. A valley is obtained when the SS ranges from 400 to 500 rev/min, and the FR ranges from 0.225 to 0.25 mm/rev. Another valley is obtained when the SS ranges from 500 to 700 rev/min, and the FR ranges from 0.1 to 0.125 mm/rev. The contour lines within the plot display curved shapes and are more concentrically spaced than parallel.

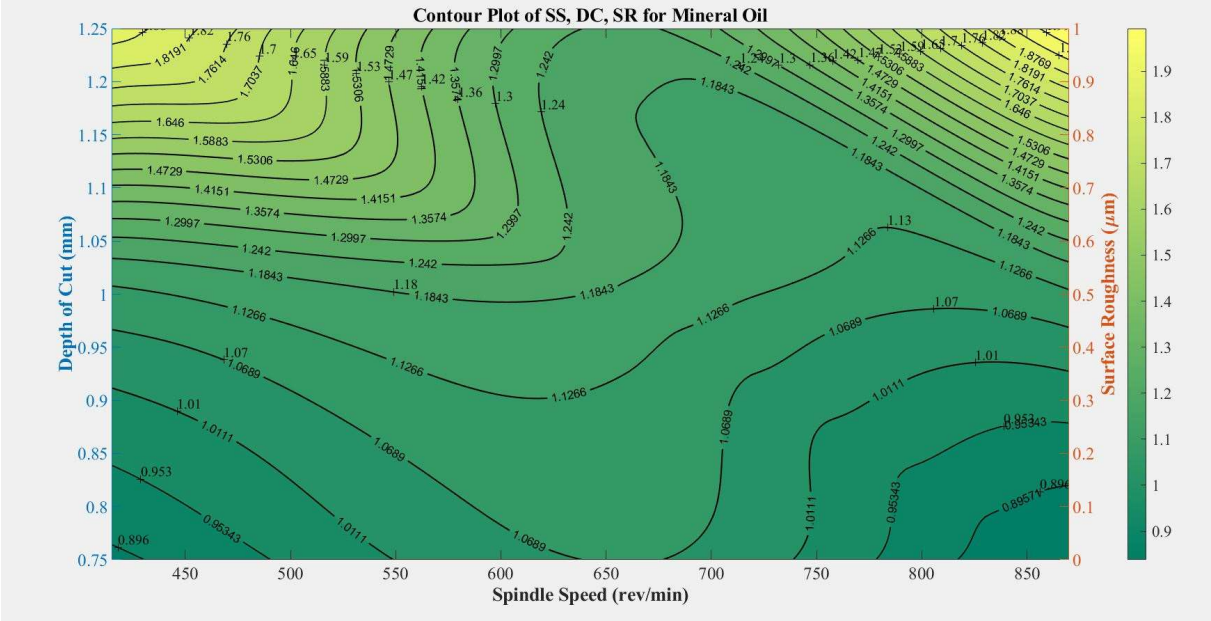

Figure 17. Contour plot of SS, DC, and SR for mineral oil.

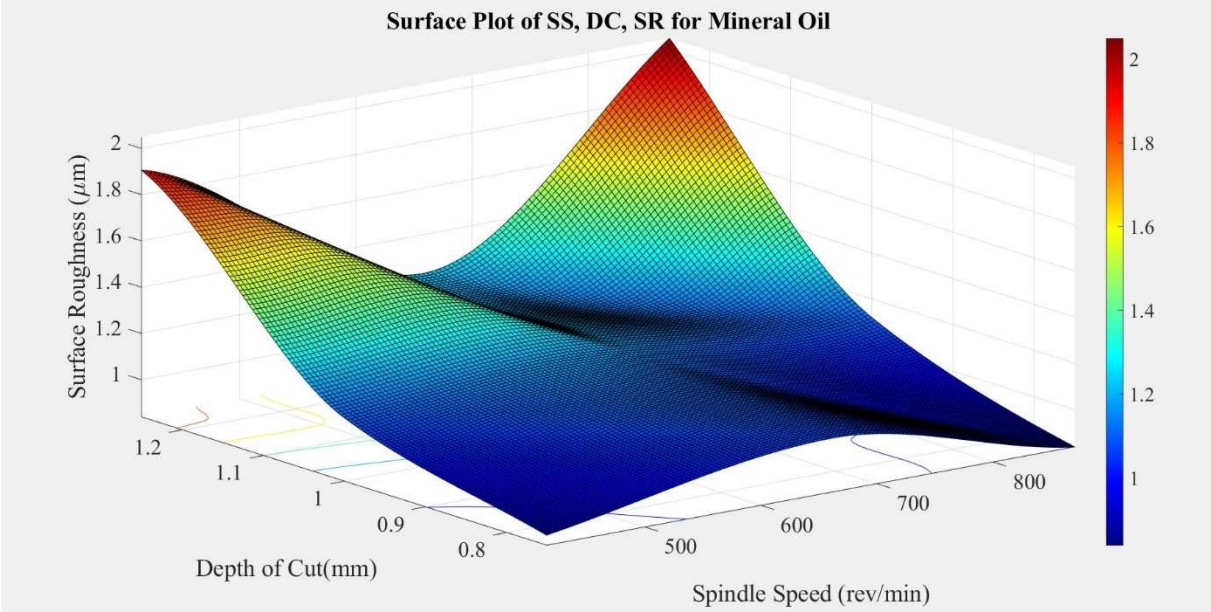

Figure 18. Surface plot of SS, DC, and SR for mineral oil.

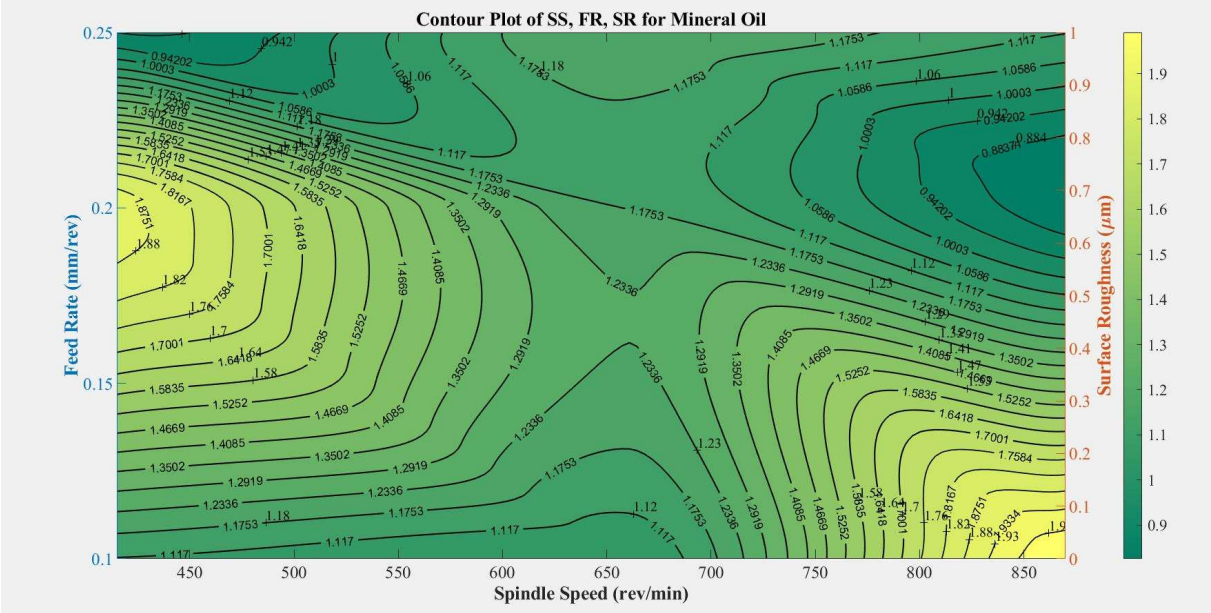

Figure 19. Contour plot of SS, FR, and SR for mineral oil.

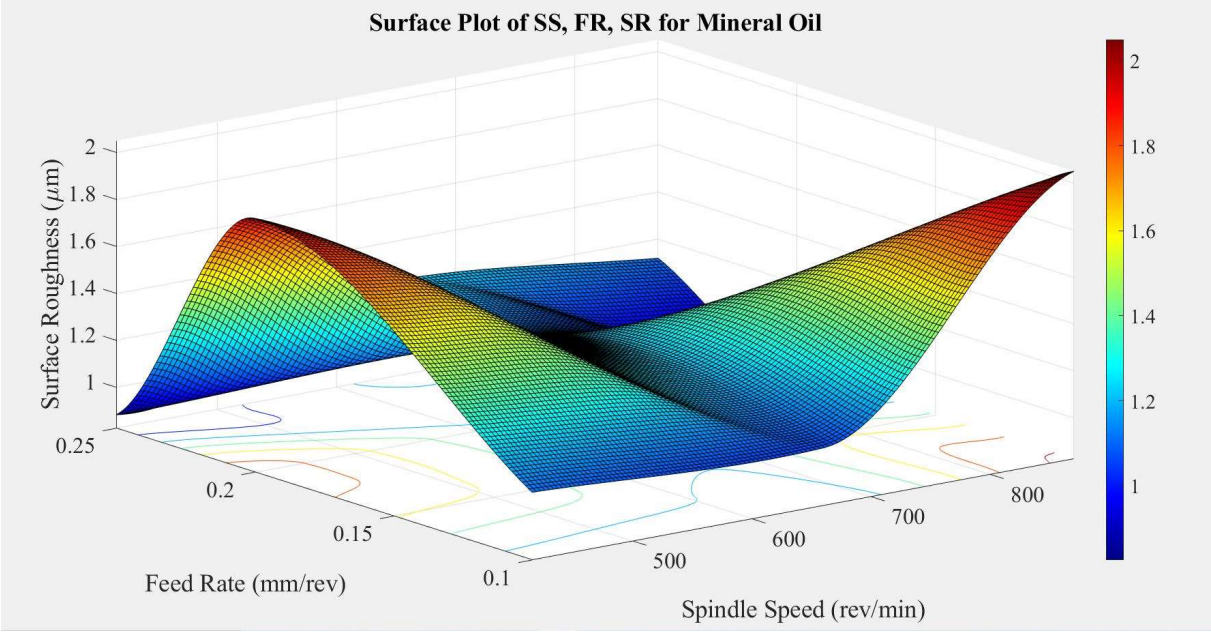

Figure 20. Surface plot of SS, FR, and SR for mineral oil.

This suggests that the SS and FR interact with each other, resulting in a combined effect on the SR that exceeds the impact of either factor acting in isolation. The non-linear and concentric nature of the contour lines indicates that adjustments to both SS and FR are necessary to effectively control and optimize SR. The surface plot depicted in Figure 20 exhibits an irregular concave shape, indicating a non-linear relationship between the SS, FR, and SR. To accurately capture this complex relationship, advanced modeling techniques such as polynomial regression, spline regression, or machine learning algorithms can be employed. The desired optimal minimum value for SR is approximately 0.95 µm, achieved when the SS is set at 450 rev/min and the FR is set at 0.25 mm/rev. Notably, the plot

demonstrates asymmetry, suggesting that SR is not equally responsive to changes in the SS and FR, regardless of the direction of adjustment [65,66]. This asymmetry implies that adjustments in either parameter will not have a comparable impact on SR. In Figure 21, the response variable is CT, while the independent variables are SS and DC. The contour lines within the plot display a parallel and linear orientation at the peak. The peak, with a CT of approximately 70 °C, occurs when the SS ranges from 800 to 850 rev/min and the DC ranges from 1.15 to 1.25 mm. This observation indicates that changes in SS and DC occur at a constant rate and act independently to influence CT, with minimal interaction between the two variables. The parallel and linear nature of the contour lines suggests that adjustments in SS and DC can be made separately and without significant consideration of their combined effect on CT. The surface plot depicted in Figure 22 exhibits a regular shape, indicating a linear relationship between the SS, DC, and CT at the region close to the peak. Observing the plot, it becomes apparent that the CT is highly sensitive to changes in the SS and DC in this specific region, as indicated by the relatively steep slope. This sensitivity implies that significant alterations in CT would be caused by small adjustments to the SS and DC [67,68].

Figure 23 illustrates a comprehensive analysis of the relationship between the independent variables, SS and FR, and their influence on the response variable, CT. Within the plot, a valley can be observed, indicating the combined effect of SS ranging from 500–700 rev/min and FR varying from 0.15–0.2 mm/rev. Notably, the highest levels of CT are associated with SS values between 800 and 900 rev/min, paired with FR ranging from 0.1–0.125 mm/rev. The contour lines exhibited in this plot demonstrate a non-linear trend, indicating that changes in the SS and FR occur at varying rates within these regions. This suggests that the interaction between SS and FR plays a significant role in influencing the CT, surpassing the impact of either factor acting in isolation. The surface plot depicted in Figure 24 displays an irregular shape, showing the relationship between the SS, FR, and CT. This irregularity suggests a non-linear correlation among these variables. To accurately capture this relationship, more advanced modeling techniques such as polynomial regression, spline regression, or machine learning algorithms can be utilized. The desired optimal minimum value for the CT is approximately 40 °C, achieved when the SS is set at 600 rev/min and the FR is set at 0.15 mm/rev. Notably, the plot exhibits symmetry on the FR axis, indicating that the CT is equally sensitive to changes in the FR, regardless of the direction of adjustment. Figure 25 showcases the relationship between the independent variables, SS and DC, and their impact on the response variable, SR. Notably, the plot reveals two distinct peaks representing high SR and a valley representing low SR. One of the peaks, characterized by an SR of approximately 6.0 μm, is achieved when the SS ranges from 400 to 600 rev/min, and the DC varies from 0.75 to 0.8 mm. Another peak, characterized by an SR of approximately 5.1 μm, is achieved when the SS ranges from 400 to 500 rev/min, and the DC varies from 1.2 to 1.25 mm. Conversely, the valley, reflecting an SR of about 2.2 μm, corresponds to an SS range of 850 to 900 rev/min, and a DC ranging from 0.80 to 1.1 mm.

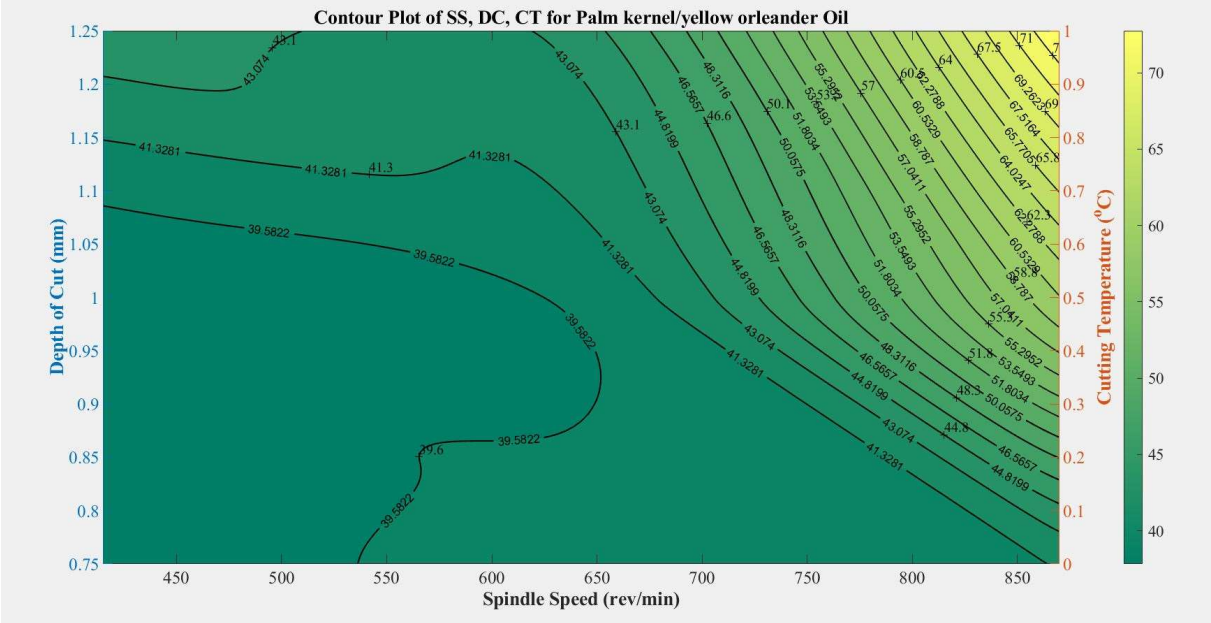

Figure 21. Contour plot of SS, DC, and CT for palm kernel + yellow orleander oil.

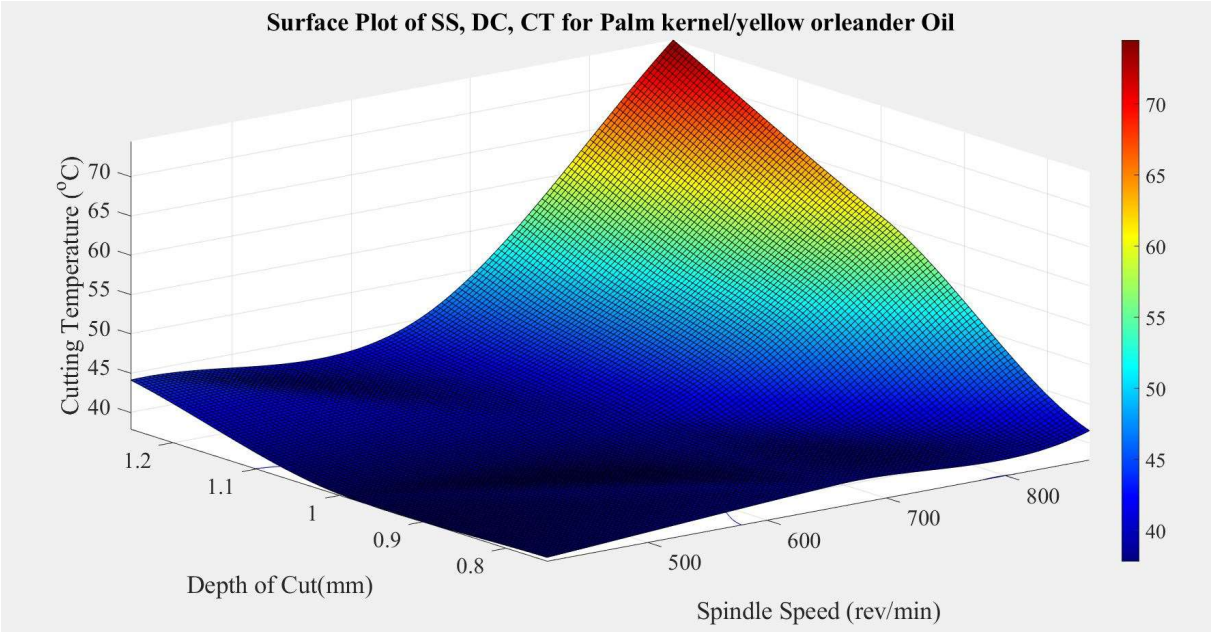

Figure 22. Surface plot of SS, DC, and CT for palm kernel + yellow orleander oil.

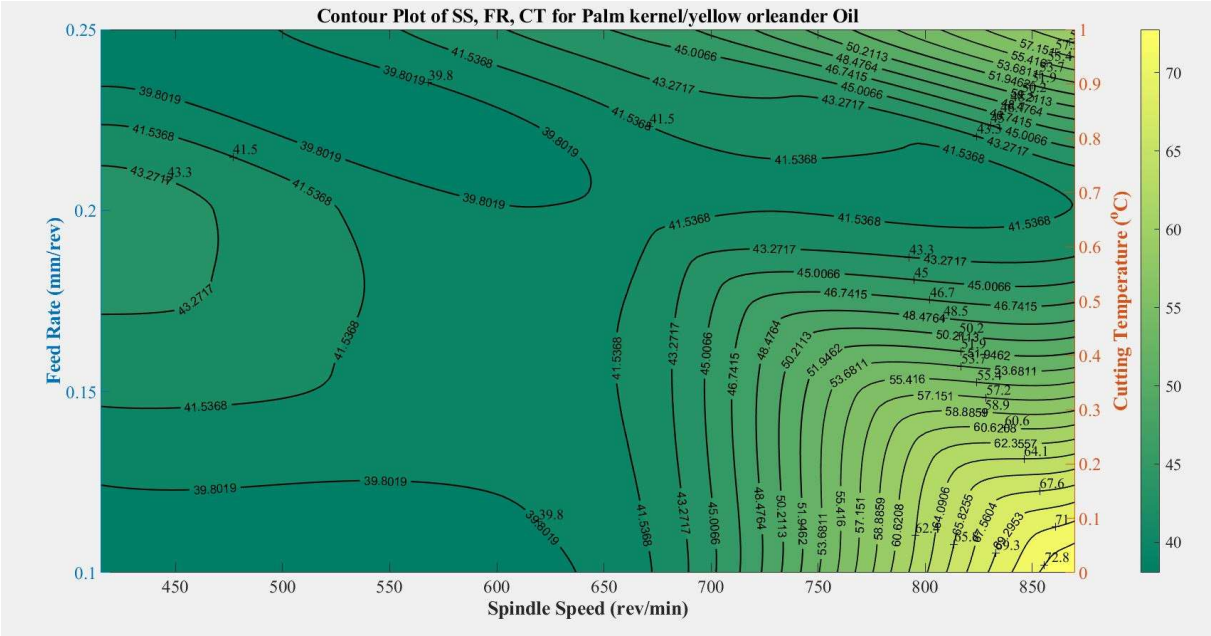

Figure 23. Contour plot of SS, FR, and CT for palm kernel + yellow orleander oil.

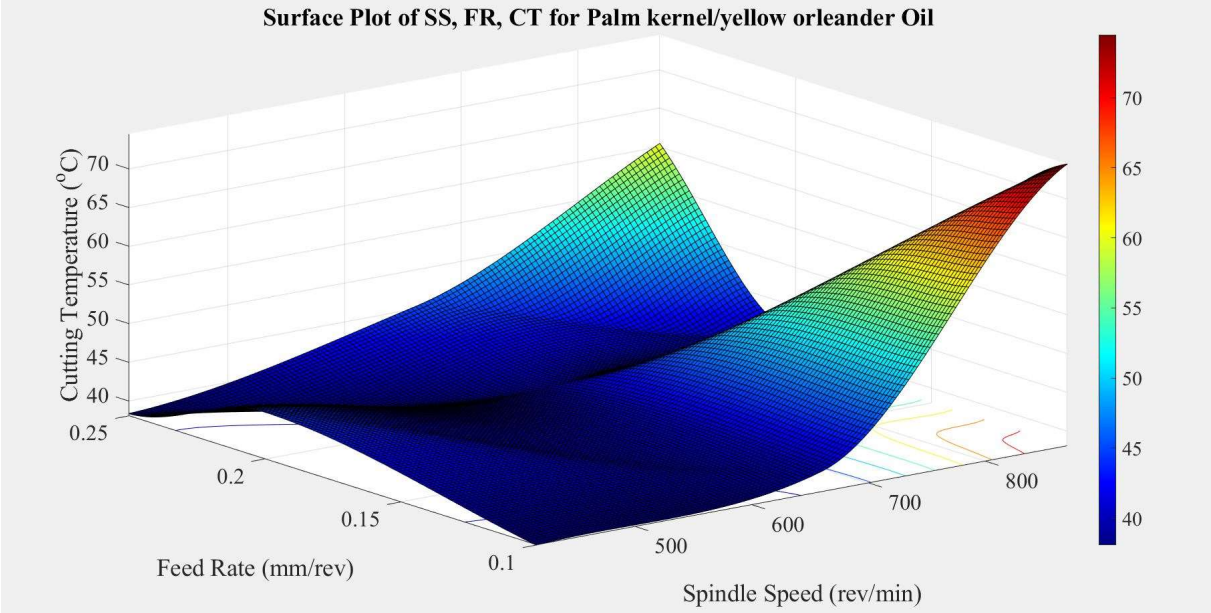

Figure 24. Surface plot of SS, FR, and CT for palm kernel + yellow orleander oil.

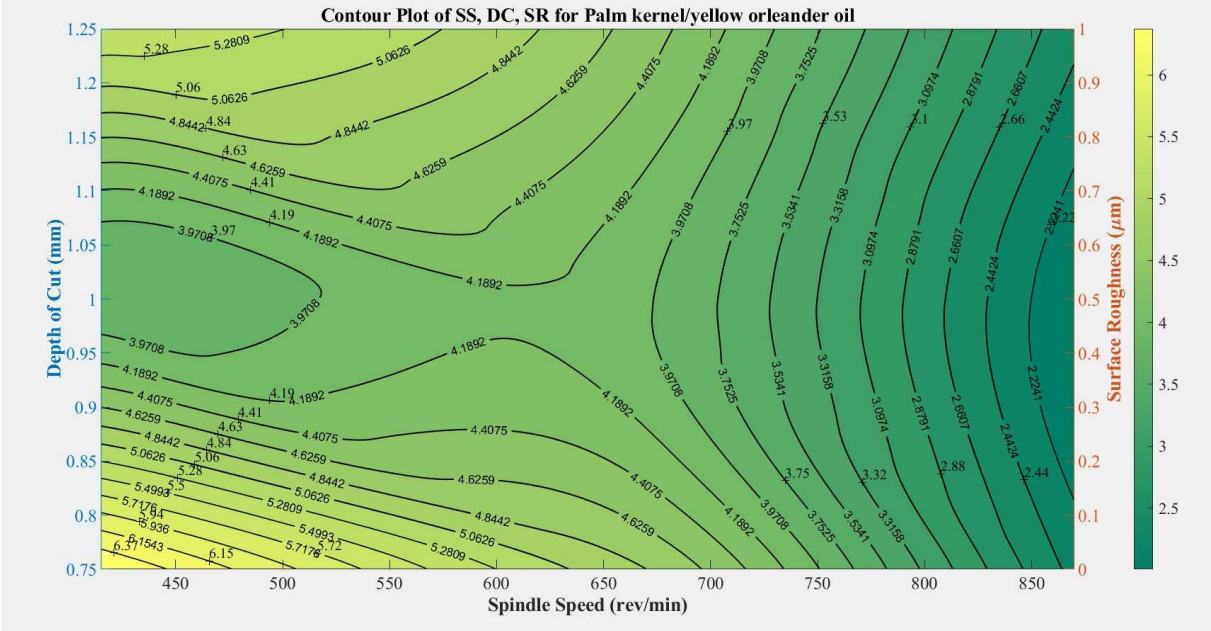

Figure 25. Contour plot of SS, DC, and SR for palm kernel + yellow orleander oil.

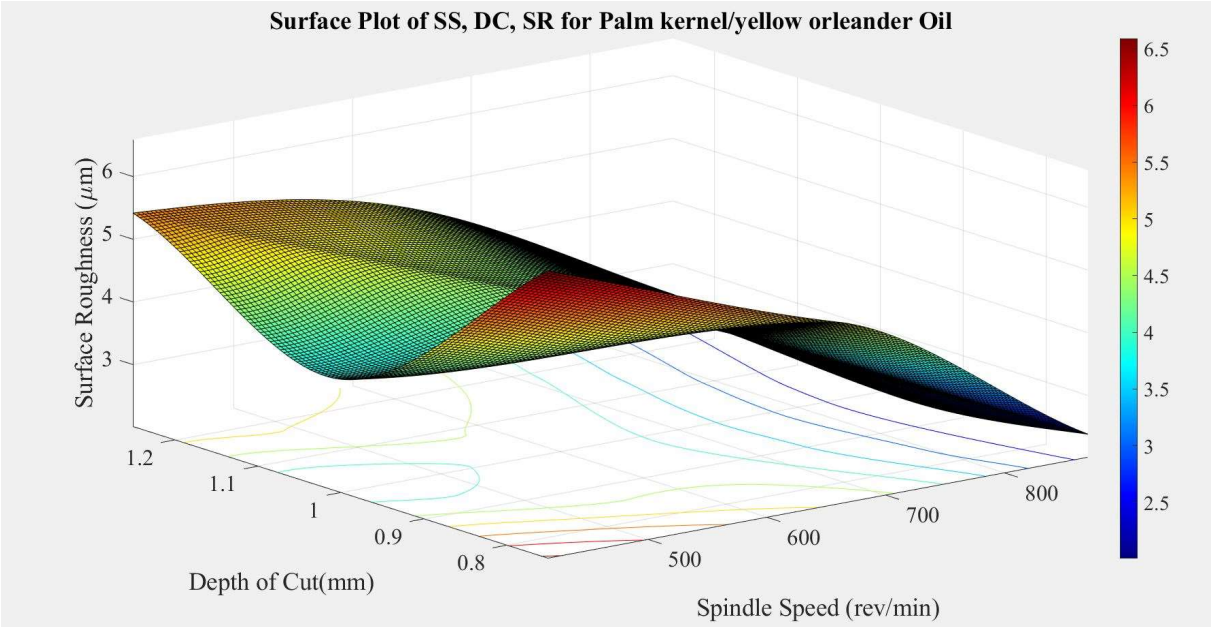

Figure 26. Surface plot of SS, DC, and SR for palm kernel + yellow orleander oil.

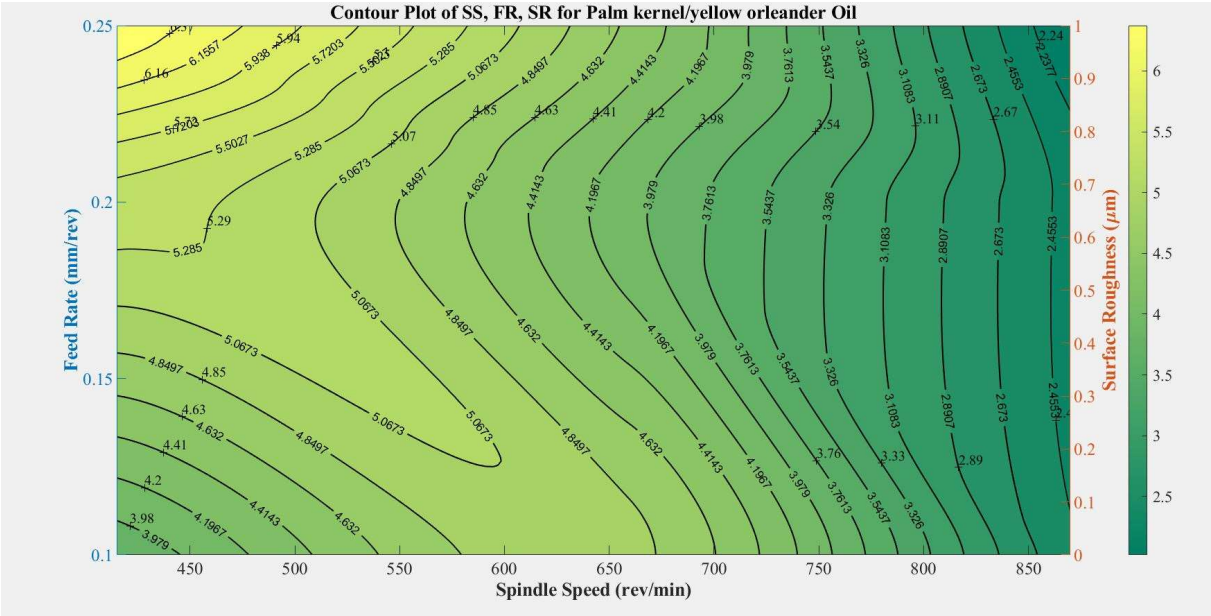

Figure 27. Contour plot of SS, FR, and SR for palm kernel + yellow orleander oil.

Examining the contour lines within the plot, they display curved shapes and are more concentrically spaced rather than parallel. This suggests that the interaction between SS and DC has a significant influence on altering the SR, surpassing the individual effects of each factor. The non-linear and concentric nature of the contour lines highlights the importance of considering the combined impact of both variables when optimizing SR. Figure 26 showcases a surface plot with an irregular convex shape, representing the relationship between the SS, DC, and SR. This shape indicates a non-linear association among these variables. Specifically, it reveals that, as the SS increases, the SR experiences a decrease, but at an increasing rate. In other words, the SR becomes more sensitive to changes in the SS as its value increases. The irregular convex shape of the plot emphasizes the non-linear nature of the relationship between the SS, DC, and SR. It suggests that careful optimization of these parameters is crucial to achieving the desired SR, as the rate of change in SR varies across different regions of the plot. In Figure 27, the response variable is SR, while the independent variables are SS and FR. The contour lines within the plot display a parallel and linear orientation at high SS values. This observation indicates that changes in SS and FR occur at a constant rate and act independently to influence SR in this region, with minimal interaction between the two variables [69,70]. The parallel and linear nature of the contour lines at this region suggests that adjustments in SS and FR can be made separately and without significant consideration of their combined effect on SR. The surface plot depicted in (Figure 28) exhibits a regular shape, indicating a linear relationship between the SS, FR, and SR. The plot highlights a minimum SR value of about 2.4 μm, achieved when the SS is in the range 850–900 rev/min. Observing the plot, it becomes apparent that the SR is highly sensitive to changes in the SS in this specific region, as indicated by the relatively steep slope. This sensitivity implies that significant alterations in SR would be caused by small adjustments in the SS. The regular shape of the surface plot emphasizes the linear relationship between the FR, SS, and SR, underscoring the importance of precise control over these variables to achieve the desired SR level.

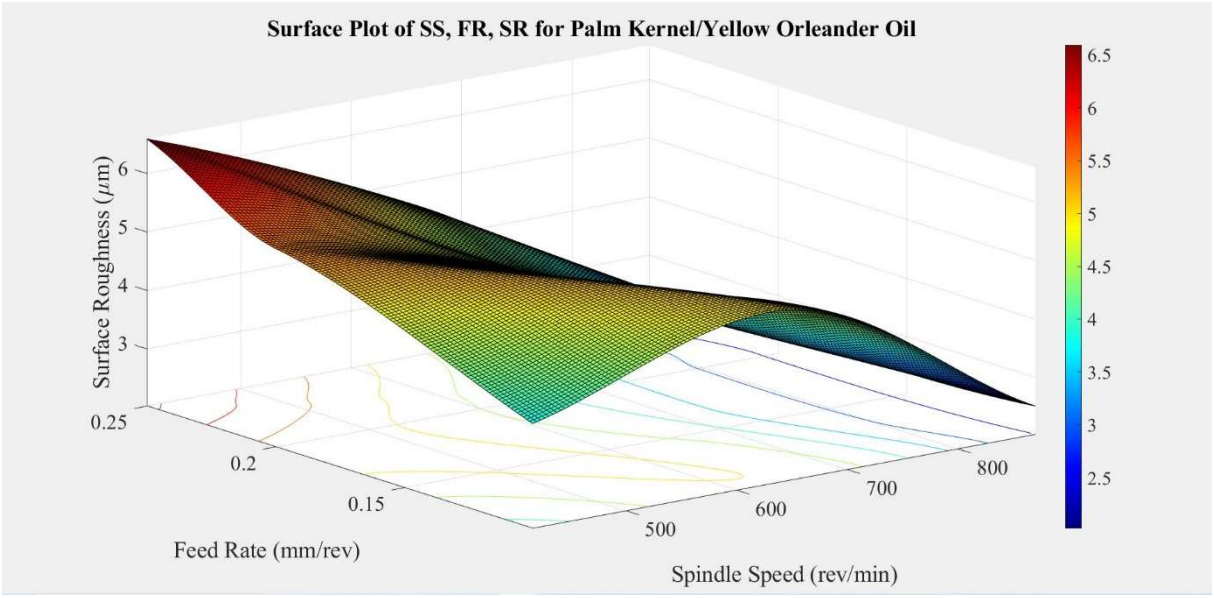

Figure 28. Surface plot of SS, FR, and SR for palm kernel + yellow orleander oil.

3.5. Main effect plots and analysis of variance

This section discusses the impact of cutting settings on response factors when turning AISI 304 stainless steel. The output line's deviation from the mean line shows which factors have the biggest impact on the turning process performance metrics. The Minitab application was used to create the main effect charts. Figure 29 illustrates the greater relevance of FR (0.25 mm/rev), DC (0.75 mm), and SS (415 rev/min) on SR for hybrid cutting fluid. As seen in Figure 30, it was discovered that the effects of spindle speed, feed rate, and DC on CT for hybrid vegetable oil were contrary to those on SR. The ideal cutting parameters for temperature are 1.25 mm, 0.10 mm/rev, and 870 rev/min. Figures 31 and 32, respectively, display the mineral oil main effect plot for SR and CT. SR can be optimally controlled with 870 rev/min SS (level 3), 0.10 mm/rev FR (level 1), and 1.25 mm DC (level 3). Similarly, CT can be optimally controlled with 870 rev/min SS (level 3), 0.25 mm/rev FR (level 3), and 1.25 mm DC (level 3). Figures 31 and 32 respectively, display the mineral oil main effect plot for SR and CT. SR can be optimally controlled with 870 rev/min SS (level 3), 0.10 mm/rev FR (level 1), and 1.25 mm DC (level 3). Similarly, CT can be optimally controlled with 870 rev/min SS (level 3), 0.25 mm/rev FR (level 3), and 1.25 mm DC (level 3). Figure 33 shows the contribution of all input parameters on SR (hybrid vegetable). The SS has the highest contribution to SR with 76%. Similarly, the ANOVA for CT (hybrid oil) in Figure 34 displays the percentage contributions from each of the following input parameters: FR (10%), DC (26%), and SS (52%). It demonstrates that the parameters that have a greater impact on the CT are SS (52%) and DC (26%). The impact of the 10% FR on the temperature of the cutting is not as severe. For these analyses, a 95% confidence level has been indicated. Analogously, with mineral oil, DC had the most impact on SR, with 71% significance (Figure 35). With a contribution of 12% and 4%, respectively, FR and SS follow next. Lastly, SS contributed 59% to the CT using mineral oil (see Figure 36).

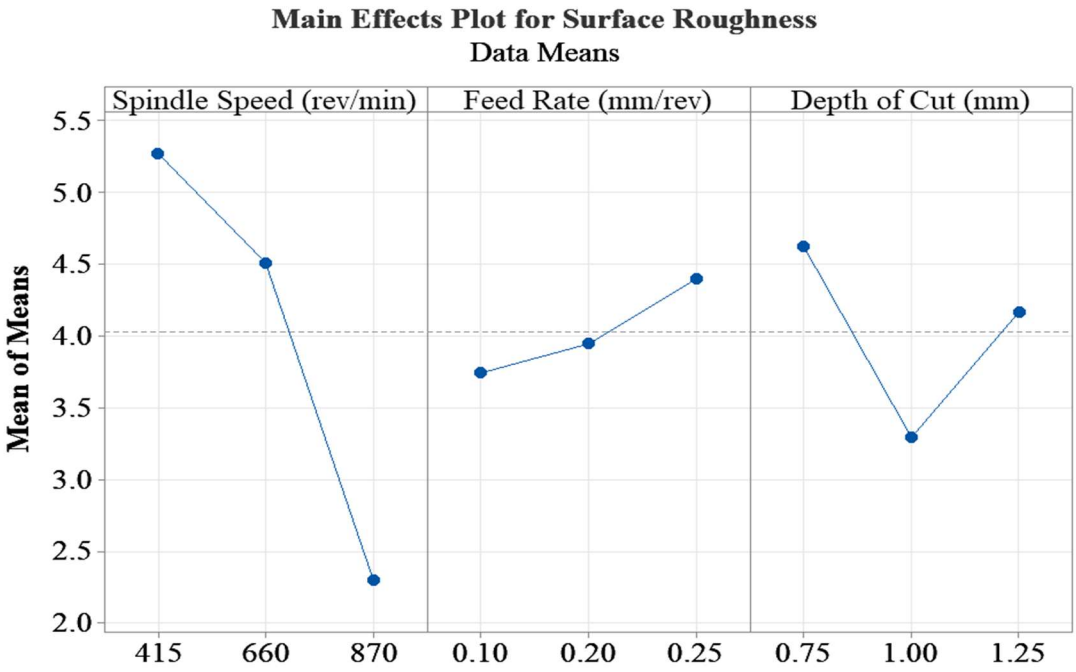

Figure 29. Main effect plot of SR for hybrid oil cutting fluid.

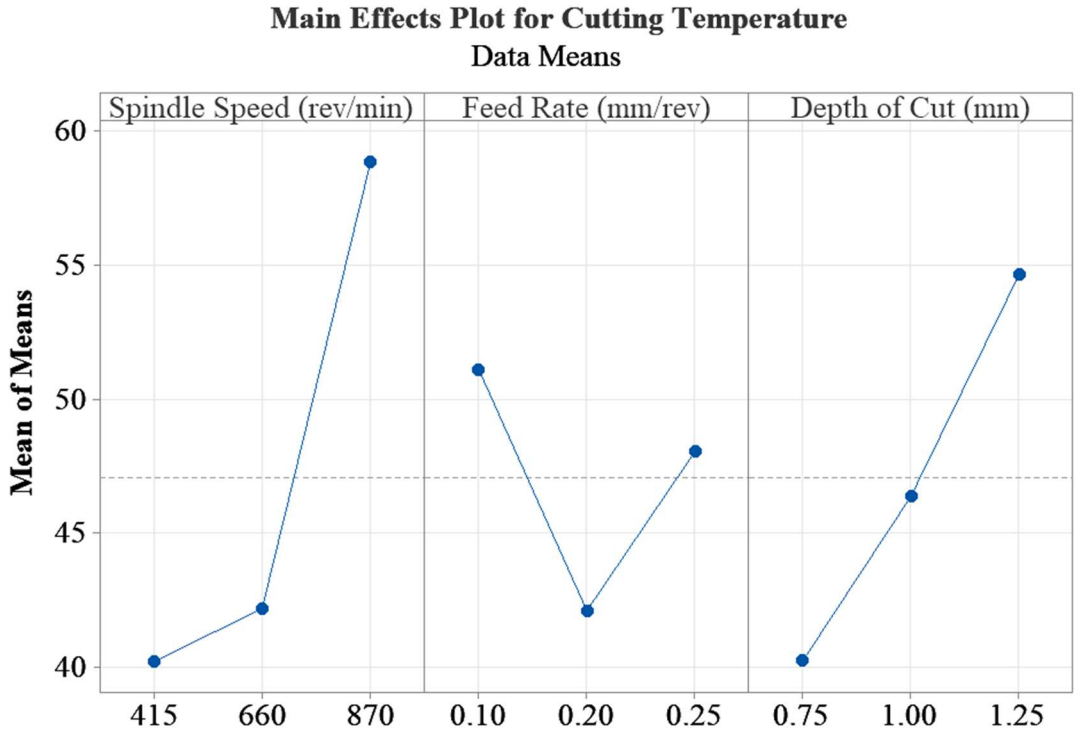

Figure 30. Main effect plot of CT for hybrid oil cutting fluid.

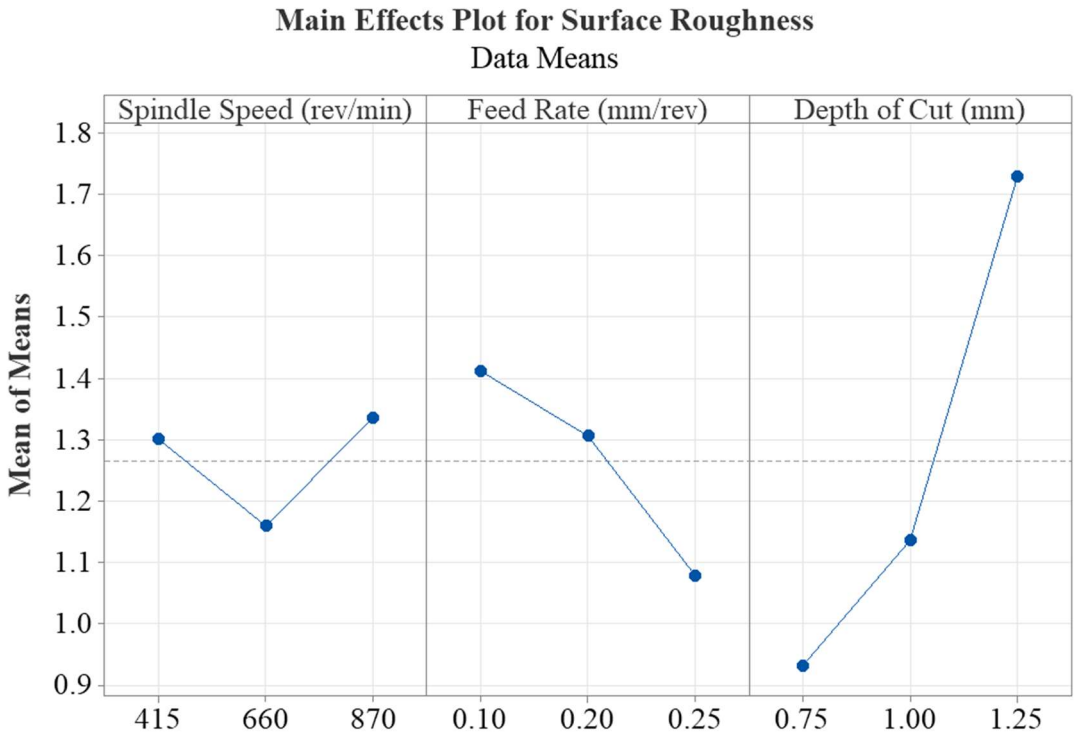

Figure 31. Main effect plot of SR for mineral oil.

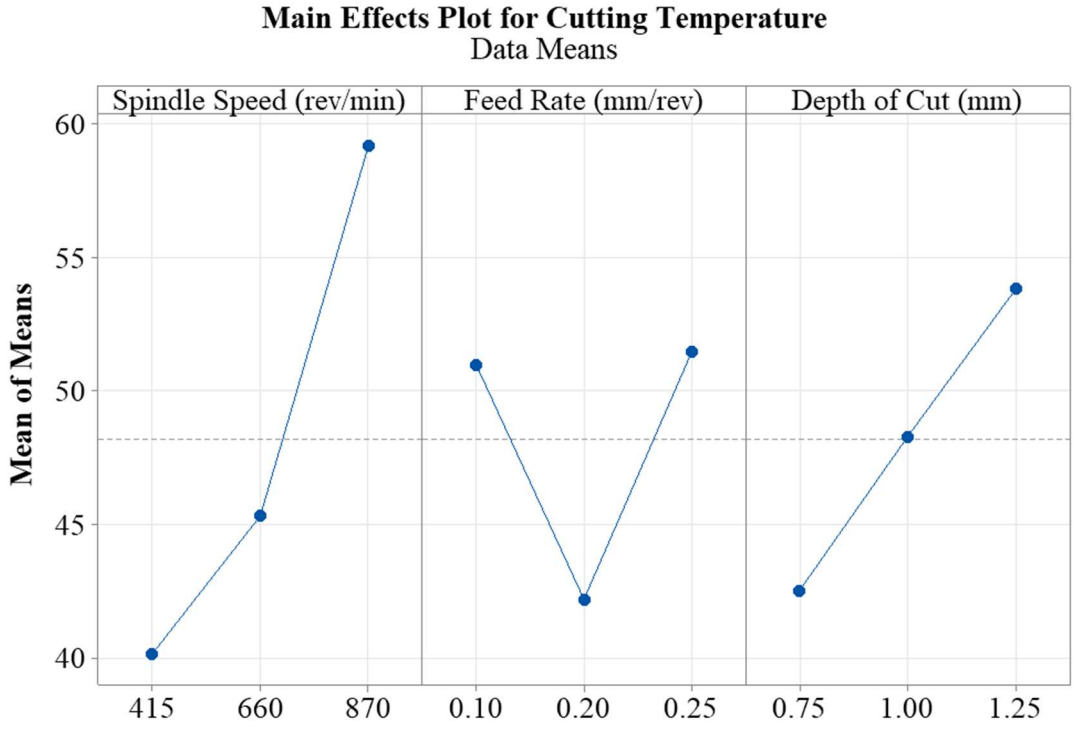

Figure 32. Main effect plot of CT for mineral oil.

Table 6. Results of ANOVA for hybrid oil lubricant.

Parameter	Source	DOF	Seq SS	Adj SS	Adj MS	F-Value	P-Value
SR (μm)	SS (rev/min)	2	14.3044	14.3044	7.1522	14.80	0.063
	FR (mm/rev)	2	0.6731	0.6731	0.3365	0.70	0.589
	DC (mm)	2	2.7481	2.7481	1.3740	2.84	0.260
	Error	2	0.9665	0.9665	0.4832	-	-
	Total	8	18.6920	-	-	-	-
CT (℃)	SS (rev/min)	2	630.2	630.2	315.11	4.38	0.186
	FR (mm/rev)	2	125.6	125.6	62.81	0.87	0.534
	DC (mm)	2	313.3	313.3	156.66	2.18	0.315
	Error	2	143.8	143.8	71.89	-	-
	Total	8	1212.9	-	-	-	-

DOF: degree of freedom; Seq SS: sequential sum of squares; Adj SS: adjusted sum of squares; Adj MS: adjusted mean squares; P-value: probability value.

Table 7. Results of ANOVA for mineral oil lubricant.

Parameter	Source	DOF	Seq SS	Adj SS	Adj MS	F-Value	P-Value
SR (μm)	SS (rev/min)	2	0.05236	0.05236	0.02618	0.28	0.781
	FR (mm/rev)	2	0.17478	0.17478	0.08739	0.93	0.517
	DC (mm)	2	1.03166	1.03166	0.51583	5.51	0.154
	Error	2	0.18729	0.18729	0.09364	-	-
	Total	8	1.44609	-	-	-	-
CT (℃)	SS (rev/min)	2	579.07	579.07	289.54	12.04	0.077
	FR (mm/rev)	2	162.94	162.94	81.47	3.39	0.228
	DC (mm)	2	190.81	190.81	95.40	3.97	0.201
	Error	2	48.11	48.11	24.05	-	-
	Total	8	980.93	-	-	-	-

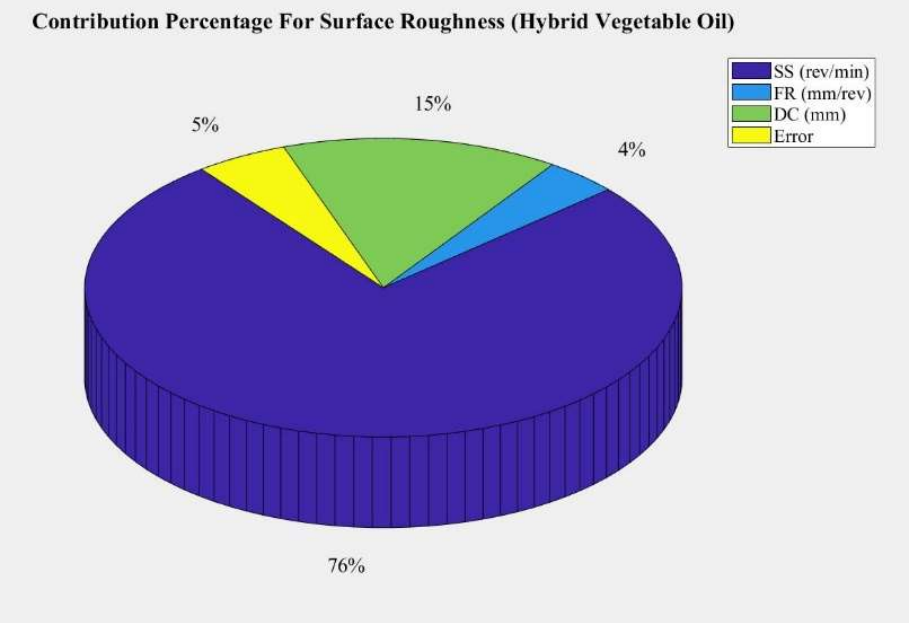

Figure 33. Contribution of process parameters for SR (hybrid oil lubricant).

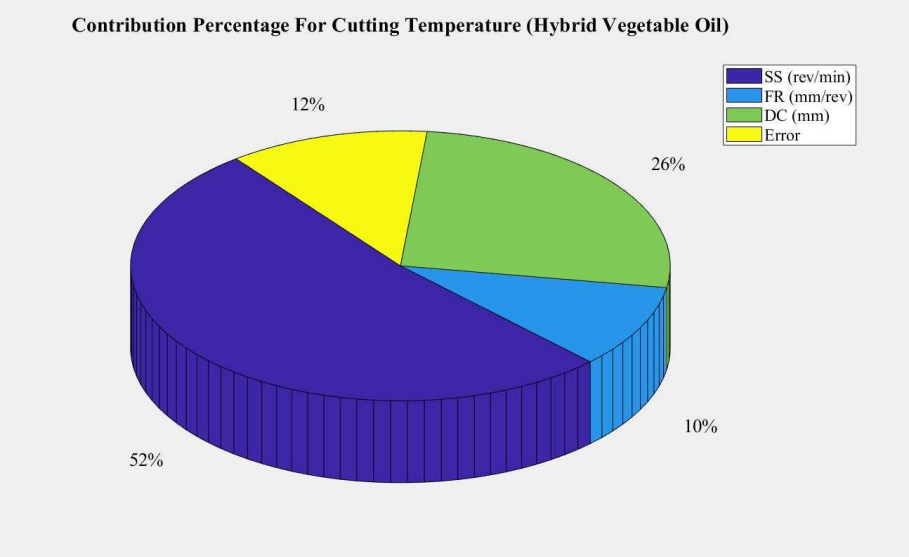

Figure 34. Contribution of process parameter to CT (hybrid oil lubricant).

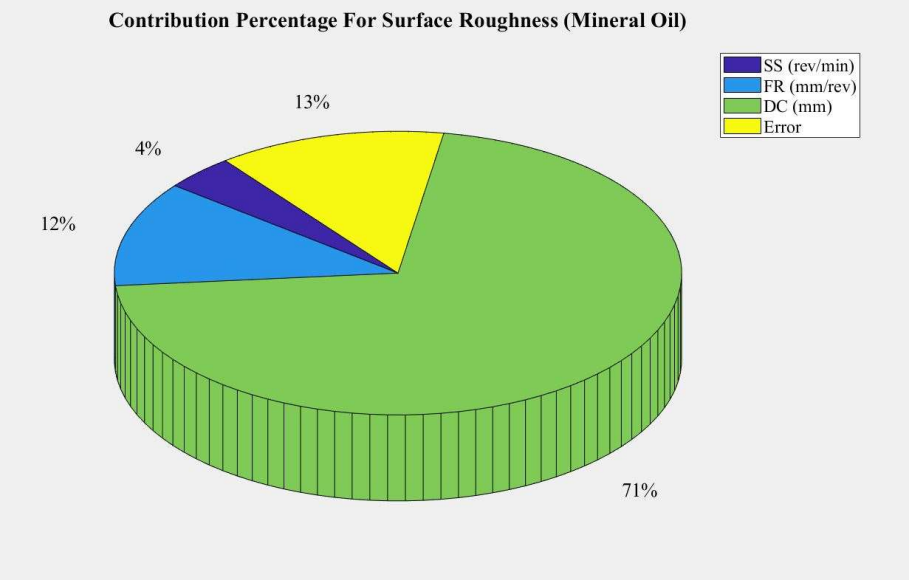

Figure 35. Contribution of process parameters for SR (mineral oil lubricant).

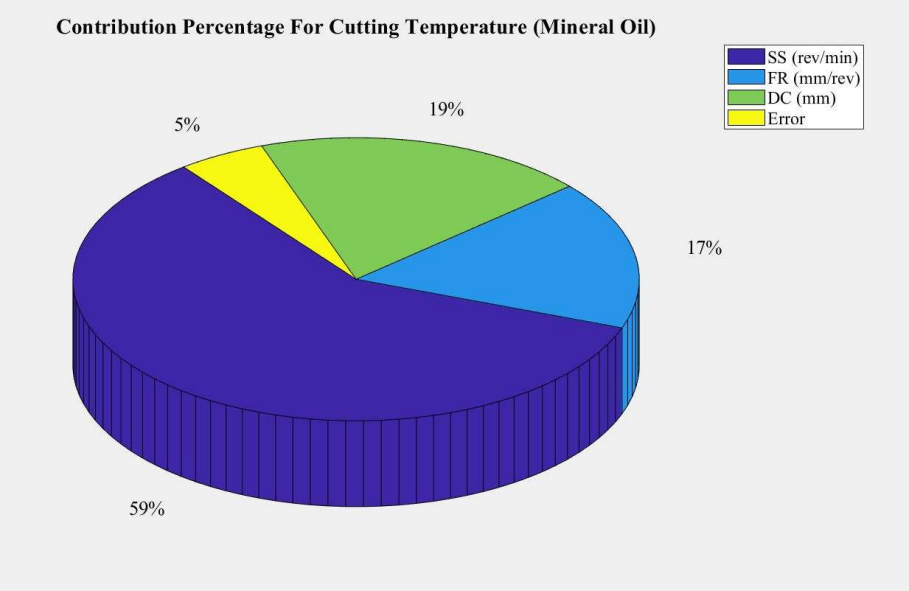

Figure 36. Contribution of process parameter to CT (mineral oil lubricant).

3.6. Regression analysis

With Minitab 17, multiple regression analysis was performed on the collected data. The DC, feed rate, and SS are the independent variables. Temperature during cutting and SR are the variables of dependence. The purpose of regression analysis is to forecast CT and SR. The resulting regression equations are shown in Eqs 1–4.

For hybrid oil cutting fluid:

$$SR(\mu m) = 4.030 - 667.9SS + 0.04705FR - 0.114DC$$
$$S = 0.6951; R^2 = 94.83\%; R^2(adj) = 79.32\% \quad (1)$$

$$CT(°C) = 47.08 - 9880.6SS - 0.354FR - 3.61DC$$
$$S = 8.4787;\ R^2 = 88.15\%; R^2(adj) = 52.58\% \quad (2)$$

For mineral oil cutting fluid:

$$SR(\mu m) = 1.265 + 5.88SS - 0.02385FR + 0.7005DC$$
$$S = 0.3060;\ R^2 = 87.05\%; R^2(adj) = 48.19\% \quad (3)$$

$$CT(°C) = 48.19 - 4265.5SS - 0.115FR + 2.82DC$$
$$S = 4.9043;\ R^2 = 95.10\%; R^2(adj) = 80.38\% \quad (4)$$

The R-Sq values for SR and CT in the case of hybrid oil lubricant are 94.83% and 88.15%, respectively. The SR and CT R-Sq values for mineral oil are 87.05% and 95.10%, respectively. In multiple linear regression analysis, the correlation coefficient, or R-Sq, should fall between 80% and 100% [27]. The findings of the experiment and the predicted ones are correlated. The R-Sq values were found to fall into a feasible range.

4. Conclusions

The performance of hybrid vegetable oil was assessed during the MQL turning operation of AISI 304 steel with an external threading tool. The effect of various cutting parameters on SR and CT was examined. The following conclusions were drawn from the study.

- The mineral oil outperformed the blend of palm kernel oil and yellow orleander oil in all SR tests.
- The hybrid cutting fluids marginally surpassed mineral oil in terms of CT.
- At low machining SS (415 rev/min), mineral oil outperformed palm kernel/yellow orleander oil by approximately 76.2% in terms of SR. At 660 rev/min and 880 rev/min, mineral oil exceeded the vegetable oil blend by 74.4% and 43.5%, respectively.
- In terms of CT, the vegetable oil mixture surpassed the mineral oil by approximately 5% and 4% at 0.75 and 1.0 mm DC.
- The SR of mineral-based oil was roughly 68.6% superior to that of the vegetable oil mixture. The palm kernel/yellow orleander oil mixture marginally outperformed mineral in terms of CT by about 2.3%.
- The results of the analysis of variance indicated that for both hybrid and mineral oil lubricants, SS had the greatest effect on CT. SS was the most significant factor influencing SR in hybrid oil, whereas DC was the most significant factor affecting SR in mineral oil.

- Hence, it is recommended that hybrid vegetable oils should be embraced as cutting fluids. This will reduce the concentration of certain species of trees. Yellow oleander oil cannot be used solely as a cutting fluid due to its congealing properties. It would perform well in a mixture with another vegetable oil with suitable properties.

Use of AI tools declaration

The authors declare that they have not used Artificial Intelligence (AI) tools in the creation of this article.

Conflict of interest

The authors declare no conflict of interest.

References

1. Maruda RW, Krolczyk GM, Nieslony P, et al. (2016) The influence of the cooling conditions on the cutting tool wear and the chip formation mechanism. *J Manuf Process* 24: 107–115. https://doi.org/10.1016/j.jmapro.2016.08.006
2. Zhu D, Zhang X, Ding H (2013) Tool wear characteristics in machining of nickel-based superalloys. *Int J Mach Tool Manu* 64: 60–77. https://doi.org/10.1016/j.ijmachtools.2012.08.001
3. Kishawy HA, Hosseini A (2019) *Machining Difficult-to-Cut Materials*, Switzerland: Springer Cham. https://doi.org/10.1007/978-3-319-95966-5
4. Abukhshim NA, Mativenga PT, Sheikh MA (2006). Heat generation and temperature prediction in metal cutting: A review and implications for high-speed machining. *Int J Mach Tool Manu* 46: 782–800. https://doi.org/10.1016/j.ijmachtools.2005.07.024
5. Wang B, Liu Z, Su G, et al. (2015) Investigations of critical cutting speed and ductile-to-brittle transition mechanism for workpiece material in ultra-high speed machining. *Int J Mech Sci* 104: 44–59. https://doi.org/10.1016/j.ijmecsci.2015.10.004
6. Prasad YVRK, Seshacharyulu TJMR (1998) Modelling of hot deformation for microstructural control. *Int Mater Rev* 43: 243–258. https://doi.org/10.1179/imr.1998.43.6.243
7. Fonda RW, Bingert JF (2004) Microstructural evolution in the heat-affected zone of a friction stir weld. *Metall Mater Trans A* 35: 1487–1499. https://doi.org/10.1007/s11661-004-0257-7
8. Kini MV, Chincholkar AM (2010) Effect of machining parameters on surface roughness and material removal rate in finish turning of ±30 glass fibre reinforced polymer pipes. *Mater Design* 31: 3590–3598. https://doi.org/10.1016/j.matdes.2010.01.013
9. Moganapriya C, Rajasekar R, Ponappa K, et al. (2018) Influence of coating material and cutting parameters on surface roughness and material removal rate in turning process using Taguchi method. *Mater Today Proc* 5: 8532–8538. https://doi.org/10.1016/j.matpr.2017.11.550
10. Daniyan IA, Tlhabadira I, Daramola OO, et al. (2019) Design and optimization of machining parameters for effective AISI P20 removal rate during milling operation. *Procedia CIRP* 84: 861–867. https://doi.org/10.1016/j.procir.2019.04.301

11. Okokpujie IP, Ohunakin OS, Bolu CA (2021) Multi-objective optimization of machining factors on surface roughness, material removal rate and cutting force on end-milling using MWCNTs nano-lubricant. *Prog Addit Manuf* 6: 155–178. https://doi.org/10.1007/s40964-020-00161-3
12. Cakir AK (2021) Analysis of surface roughness, sound level and machine current in the turning of hardened AISI S1 steel. *Trans Indian Inst Met* 74: 691–703. https://doi.org/10.1007/s12666-021-02196-8
13. Tekıner Z, Yeşılyurt S (2004) Investigation of the cutting parameters depending on process sound during turning of AISI 304 austenitic stainless steel. *Mater Design* 25: 507–513. https://doi.org/10.1016/j.matdes.2003.12.011
14. Şahinoğlu A, Güllü A (2020) Investigation of the relationship between current, sound intensity, vibration and surface roughness in machining of CuZn39Pb3 material on lathe machine. *J Polytech* 23: 615–624. http://doi.org/10.2339/politeknik.426106
15. Fedai Y (2023) Exploring the impact of the turning of AISI 4340 steel on tool wear, surface roughness, sound intensity, and power consumption under dry, MQL, and nano-MQL conditions. *Lubricants* 11: 442. https://doi.org/10.3390/lubricants11100442
16. Rafighi M, Özdemir M, Şahinoğlu A, et al. (2022) Experimental assessment and topsis optimization of cutting force, surface roughness, and sound intensity in hard turning of AISI 52100 steel. *Surf Rev Lett* 29: 2250150. https://doi.org/10.1142/S0218625X22501505
17. Mia M, Dey PR, Hossain MS, et al. (2018) Taguchi S/N based optimization of machining parameters for surface roughness, tool wear and material removal rate in hard turning under MQL cutting condition. *Measurement* 122: 380–391. https://doi.org/10.1016/j.measurement.2018.02.016
18. Kazeem RA, Fadare DA, Ikumapayi OM, et al. (2022) Advances in the application of vegetable-oil-based cutting fluids to sustainable machining operations—a review. *Lubricants* 10: 69. https://doi.org/10.3390/lubricants10040069
19. Yin Q, Li C, Dong L, et al. (2021) Effects of physicochemical properties of different base oils on friction coefficient and surface roughness in MQL milling AISI 1045. *Int J Pr Eng Man-GT* 8: 1629–1647. https://doi.org/10.1007/s40684-021-00318-7
20. Sharma J, Sidhu BS (2014) Investigation of effects of dry and near dry machining on AISI D2 steel using vegetable oil. *J Clean Prod* 66: 619–623. https://doi.org/10.1016/j.jclepro.2013.11.042
21. Kuram E, Ozcelik B, Demirbas E, et al. (2011) Evaluation of new vegetable-based cutting fluids on thrust force and surface roughness in drilling of AISI 304 using Taguchi method. *Mater Manuf Process* 26: 1136–1146. https://doi.org/10.1080/10426914.2010.536933
22. Xavior MA, Adithan M (2009) Determining the influence of cutting fluids on tool wear and surface roughness during turning of AISI 304 austenitic stainless steel. *J Mater Process Technol* 209: 900–909. https://doi.org/10.1016/j.jmatprotec.2008.02.068
23. Bai X, Zhou F, Li C, et al. (2020) Physicochemical properties of degradable vegetable-based oils on minimum quantity lubrication milling. *Int J Adv Manuf Technol* 106: 4143–4155. https://doi.org/10.1007/s00170-019-04695-x
24. Saleem MQ, Mehmood A (2022) Eco-friendly precision turning of superalloy Inconel 718 using MQL based vegetable oils: Tool wear and surface integrity evaluation. *J Manuf Process* 73: 112–127. https://doi.org/10.1016/j.jmapro.2021.10.059

25. Shankar S, Manikandan M, Raja G, et al. (2020) Experimental investigations of vibration and acoustics signals in milling process using kapok oil as cutting fluid. *Mech Ind* 21: 521. https://doi.org/10.1051/meca/2020066
26. Sen B, Gupta MK, Mia M, et al. (2021). Performance assessment of minimum quantity castor-palm oil mixtures in hard-milling operation. *Materials* 14: 198. https://doi.org/10.3390/ma14010198
27. Kazeem RA, Fadare DA, Abutu J, et al. (2020) Performance evaluation of jatropha oil-based cutting fluid in turning AISI 1525 steel alloy. *CIRP J Manuf Sci Tec* 31: 418–430. https://doi.org/10.1016/j.cirpj.2020.07.004
28. Baderna D, Lomazzi E, Passoni A, et al. (2015) Chemical characterization and ecotoxicity of three soil foaming agents used in mechanized tunneling. *J Hazard Mater* 296: 210–220. https://doi.org/10.1016/j.jhazmat.2015.04.040
29. Alaba ES, Kazeem RA, Adebayo AS, et al. (2023) Evaluation of palm kernel oil as cutting lubricant in turning AISI 1039 steel using Taguchi-grey relational analysis optimization technique. *Adv Ind Manuf Eng* 6: 100115. https://doi.org/10.1016/j.aime.2023.100115
30. Ikumapayi OM, Kazeem RA, Ogedengbe TS, et al. (2023) Performance evaluation of African star seed (chrysophyllum albidum) oil as a cutting lubricant in milling of ASTM A36 steel. *Adv Mater Process Te* 1–15. https://doi.org/10.1080/2374068X.2023.2192391
31. Kazeem RA, Enobun IO, Akande IG, et al. (2023) Evaluation of palm kernel oil as lubricants in cylindrical turning of AISI 304 austenitic stainless steel using Taguchi-grey relational methodology. *Mater Res Express* 10: 126505. https://doi.org/10.1088/2053-1591/ad11fe
32. Abegunde PO, Kazeem RA, Akande IG, et al. (2023) Performance assessment of some selected vegetable oils as lubricants in turning of AISI 1045 steel using a Taguchi-based grey relational analysis approach. *Tribol-Mater Surf In* 17: 187–202. https://doi.org/10.1080/17515831.2023.2235227
33. Said Z, Gupta M, Hegab H, et al. (2019) A comprehensive review on minimum quantity lubrication (MQL) in machining processes using nano-cutting fluids. *Int J Adv Manuf Tech* 105: 2057–2086. https://doi.org/10.1007/s00170-019-04382-x
34. Tazehkandi AH, Shabgard M, Pilehvarian F (2015) On the feasibility of a reduction in cutting fluid consumption via spray of biodegradable vegetable oil with compressed air in machining Inconel 706. *J Clean Prod* 104: 422–435. https://doi.org/10.1016/j.jclepro.2015.05.039
35. Sarıkaya M, Gupta MK, Tomaz I, et al. (2021) A state-of-the-art review on tool wear and surface integrity characteristics in machining of superalloys. *CIRP J Manuf Sci Tec* 35: 624–658. https://doi.org/10.1016/j.cirpj.2021.08.005
36. Usca UA, Uzun M, Kuntoğlu M, et al. (2021) Investigations on tool wear, surface roughness, cutting temperature, and chip formation in machining of Cu-B-CrC composites. *Int J Adv Manuf Tech* 116: 3011–3025. https://doi.org/10.1007/s00170-021-07670-7
37. Liu D, Liu Z, Zhao J, et al. (2022) Tool wear monitoring through online measured cutting force and cutting temperature during face milling Inconel 718. *Int J Adv Manuf Tech* 122: 729–740. https://doi.org/10.1007/s00170-022-09950-2
38. Rajaguru J, Arunachalam N (2020) A comprehensive investigation on the effect of flood and MQL coolant on the machinability and stress corrosion cracking of super duplex stainless steel. *J Mater Process Technol* 276: 116417. https://doi.org/10.1016/j.jmatprotec.2019.116417

39. Yasir M, Danish M, Mia M, et al. (2021). Investigation into the surface quality and stress corrosion cracking resistance of AISI 316L stainless steel via precision end-milling operation. *Int J Adv Manuf Tech* 112: 1065–1076. https://doi.org/10.1007/s00170-020-06413-4
40. Hegab H, Umer U, Soliman M, et al. (2018) Effects of nano-cutting fluids on tool performance and chip morphology during machining Inconel 718. *Int J Adv Manuf Tech* 96: 3449–3458. https://doi.org/10.1007/s00170-018-1825-0
41. Liew PJ, Shaaroni A, Sidik NAC, et al. (2017) An overview of current status of cutting fluids and cooling techniques of turning hard steel. *Int J Heat Mass Tran* 114: 380–394. https://doi.org/10.1016/j.ijheatmasstransfer.2017.06.077
42. Aramesh M, Montazeri S, Veldhuis SC (2018) A novel treatment for cutting tools for reducing the chipping and improving tool life during machining of Inconel 718. *Wear* 414: 79–88. https://doi.org/10.1016/j.wear.2018.08.002
43. Debnath S, Reddy MM, Yi QS (2016) Influence of cutting fluid conditions and cutting parameters on surface roughness and tool wear in turning process using Taguchi method. *Measurement* 78: 111–119. https://doi.org/10.1016/j.measurement.2015.09.011
44. Nasirudeen AR, Lasisi D, Balogun LA (2019) Physico-chemical properties of yellow oleander (Thevetia peruviana) and their effects on the qualities of biodiesel. *Arid Zone J Eng Tech Env* 15: 859–866. Available from: https://www.azojete.com.ng/index.php/azojete/article/view/140.
45. Bachchhav B, Bagchi H (2021) Effect of surface roughness on friction and lubrication regimes. *Mater Today Proc* 38: 169–173. https://doi.org/10.1016/j.matpr.2020.06.252
46. Oliaei SNB, Karpat Y (2016) Investigating the influence of built-up edge on forces and surface roughness in micro scale orthogonal machining of titanium alloy Ti6Al4V. *J Mater Process Technol* 235: 28–40. https://doi.org/10.1016/j.jmatprotec.2016.04.010
47. Meddour I, Yallese MA, Khattabi R (2015) Investigation and modeling of cutting forces and surface roughness when hard turning of AISI 52100 steel with mixed ceramic tool: Cutting conditions optimization. *Int J Adv Manuf Tech* 77: 1387–1399. https://doi.org/10.1007/s00170-014-6559-z
48. Mikolajczyk T (2014) Modeling of minimal thickness cutting layer influence on surface roughness in turning. *Appl Mech Mater* 656: 262–269. https://doi.org/10.4028/www.scientific.net/AMM.656.262
49. Akhtar W, Sun J, Chen W (2016) Effect of machining parameters on surface integrity in high speed milling of super alloy GH4169/Inconel 718. *Mater Manuf Process* 31: 620–627. https://doi.org/10.1080/10426914.2014.994769
50. Uddin MS, Rosman H, Hall C (2017) Enhancing the corrosion resistance of biodegradable Mg-based alloy by machining-induced surface integrity: Influence of machining parameters on surface roughness and hardness. *Int J Adv Manuf Tech* 90: 2095–2108. https://doi.org/10.1007/s00170-016-9536-x
51. Su G, Xiao X, Du J (2020). On cutting temperatures in high and ultrahigh-speed machining. *Int J Adv Manuf Tech* 107: 73–83. https://doi.org/10.1007/s00170-020-05054-x
52. Zhang X, Peng Z, Li Z, et al. (2020) Influences of machining parameters on tool performance when high-speed ultrasonic vibration cutting titanium alloys. *J Manuf Process* 60: 188–199. https://doi.org/10.1016/j.jmapro.2020.10.053

53. Kartal F, Yerlikaya Z, Okkaya H (2017) Effects of machining parameters on surface roughness and macro surface characteristics when the machining of Al-6082 T6 alloy using AWJT. *Measurement* 95: 216–222. https://doi.org/10.1016/j.measurement.2016.10.007
54. Diniardi E, Yudistirani SA, Basri H, et al. (2021) Analysis of the effect of cutting variables against surface hardness. *J Appl Sci Adv Tech* 3: 81–88. https://doi.org/10.24853/jasat.3.3.81-88
55. Pang X, Zhang Y, Wang C, et al. (2020) Effect of cutting parameters on cutting force and surface quality in cutting of articular cartilage. *Procedia CIRP* 89: 116–121. https://doi.org/10.1016/j.procir.2020.05.127
56. Majak D, Olugu EU, Lawal SA (2020) Analysis of the effect of sustainable lubricants in the turning of AISI 304 stainless steel. *Procedia Manuf* 43: 495–502. https://doi.org/10.1016/j.promfg.2020.02.183
57. Xavior MA, Adithan M (2009) Determining the influence of cutting fluids on tool wear and surface roughness during turning of AISI 304 austenitic stainless steel. *J Mater Process Technol* 209: 900–909. https://doi.org/10.1016/j.jmatprotec.2008.02.068
58. Sarıkaya M, Yılmaz V, Gullu A (2016) Analysis of cutting parameters and cooling/lubrication methods for sustainable machining in turning of Haynes 25 superalloy. *J Clean Prod* 133: 172–181. https://doi.org/10.1016/j.jclepro.2016.05.122
59. Manjunath K, Tewary S, Khatri N, et al. (2021) Monitoring and predicting the surface generation and surface roughness in ultraprecision machining: A critical review. *Machines* 9: 369. https://doi.org/10.3390/machines9120369
60. Chakraborty P, Asfour S, Cho S, et al. (2008) Modeling tool wear progression by using mixed effects modeling technique when end-milling AISI 4340 steel. *J Mater Process Technol* 205: 190–202. https://doi.org/10.1016/j.jmatprotec.2007.11.197
61. Flynn JM, Shokrani A, Newman ST, et al. (2016) Hybrid additive and subtractive machine tools—Research and industrial developments. *Int J Mach Tool Manu* 101: 79–101. https://doi.org/10.1016/j.ijmachtools.2015.11.007
62. Dabees S, Mirzaei S, Kaspar P, et al. (2022) Characterization and evaluation of engineered coating techniques for different cutting tools. *Materials* 15: 5633. https://doi.org/10.3390/ma15165633
63. Yeganefar A, Niknam SA, Asadi R (2019) The use of support vector machine, neural network, and regression analysis to predict and optimize surface roughness and cutting forces in milling. *Int J Adv Manuf Technol* 105: 951–965. https://doi.org/10.1007/s00170-019-04227-7
64. Praveen N, Mallik US, Shivasiddaramaiah AG, et al. (2023) Effect of CNC end milling parameters on Cu-Al-Mn ternary shape memory alloys using Taguchi method. *J Inst Eng India Ser D* https://doi.org/10.1007/s40033-023-00579-3
65. Guo Y, Yang X, Kang J, et al. (2022) Ductile machining of single-crystal germanium for freeform surfaces diamond turning based on a long-stroke fast tool servo. *J Manuf Process* 82: 615–627. https://doi.org/10.1016/j.jmapro.2022.08.013
66. Patange AD, Jegadeeshwaran R (2021) Review on tool condition classification in milling: A machine learning approach. *Mater Today Proc* 46: 1106–1115. https://doi.org/10.1016/j.matpr.2021.01.523
67. Saglam H, Yaldiz S, Unsacar F (2007) The effect of tool geometry and cutting speed on main cutting force and tool tip temperature. *Mater Design* 28: 101–111. https://doi.org/10.1016/j.matdes.2005.05.015

68. Sheikh-Ahmad JY, Almaskari F, Hafeez F (2019) Thermal aspects in machining CFRPs: Effect of cutter type and cutting parameters. *Int J Adv Manuf Tech* 100: 2569–2582. https://doi.org/10.1007/s00170-018-2881-1
69. Käsemodel RB, De Souza AF, Voigt R, et al. (2020) CAD/CAM interfaced algorithm reduces cutting force, roughness, and machining time in free-form milling. *Int J Adv Manuf Tech* 107: 1883–1900. https://doi.org/10.1007/s00170-020-05143-x
70. Safiei W, Rahman MM, Yusoff AR, et al. (2021) Effects of SiO2-Al_2O_3-ZrO_2 tri-hybrid nanofluids on surface roughness and cutting temperature in end milling process of aluminum alloy 6061-T6 using uncoated and coated cutting inserts with minimal quantity lubricant method. *Arab J Sci Eng* 46: 7699–7718. https://doi.org/10.1007/s13369-021-05533-7

AIMS Press